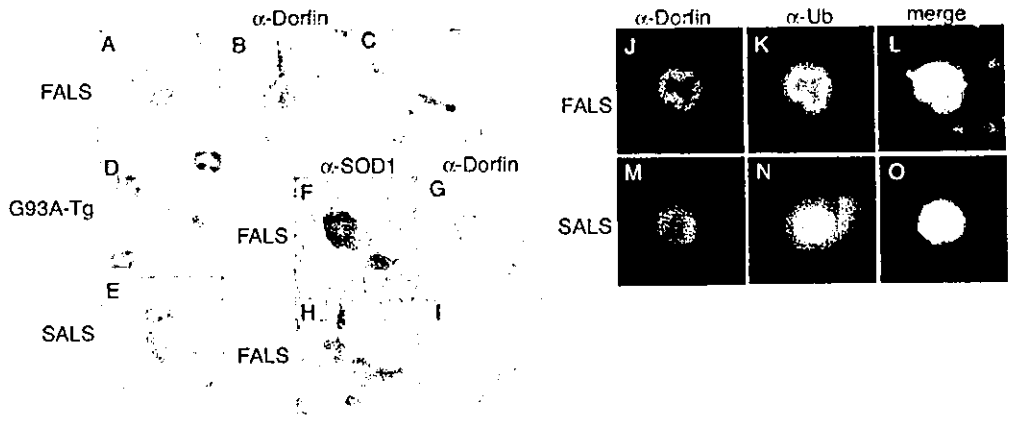

FIG. 1. **Localization of Dorfin in inclusion bodies in spinal cord motor neurons of ALS and mutant SOD1-transgenic mice.** The transverse sections of the spinal cord from familial ALS (*FALS, panels A–C*), $SOD1^{G93A}$-transgenic mice (*G93A-Tg, panel D*), and sporadic ALS (*SALS, panel E*) were immunohistochemically stained with the anti-Dorfin antibody. The hyaline inclusions in familial ALS were stained with anti-SOD1 (*α-SOD1, panels F* and *H*) or anti-Dorfin (*α-Dorfin, panels G* and *I*) antibodies. Note that *panels F* and *G* or *H* and *I* are the identical sections doubly immunostained. Spinal cord sections from familial (*panels J–L*) and sporadic (*panels M–O*) ALS were double labeled by indirect immunofluorescence with anti-Dorfin antibody (*panels J* and *M*) and monoclonal antibody to Ub (*α-UB, panels K* and *N*) and observed by a laser-scanning confocal microscope. *Panel L* is *panels J* and *K* merged; *panel O* is *panels M* and *N* merged. Magnification, ×225 (*panels A–C, E* and *F–I*) and ×675 (*panels D* and *J–O*).

genic mice and is involved in the ubiquitylation and targeted degradation of mutant SOD1.

EXPERIMENTAL PROCEDURES

Immunohistochemistry—Immunohistochemical studies were carried out on 10% formalin-fixed, paraffin-embedded spinal cords filed in the Department of Neurology, Nagoya University Graduate School of Medicine. The specimens were obtained at autopsy from two familial ALS patients with mutant $SOD1^{N86S}$ (male aged 57 years and female aged 54 years), three sporadic cases of ALS (all males, aged 46, 59, and 67 years) and four age-matched, non-neurologic disease patients. The spinal cord specimens of these ALS cases and those of mutant $SOD1^{G93A}$-transgenic mice (B6SJL-TgN(SOD1-G93A)1Gur; The Jackson Laboratory) were immunohistochemically stained with antibodies against Dorfin (14), SOD1 (SOD-100; StressGen Biotechnologies, La Jolla, CA), and Ub (P4D1; Santa Cruz Biotechnology). Double staining of identical sections was performed as described (31). In immunofluorescence microscopy, Alexa-488- and Alexa-546-conjugated secondary antibodies (Molecular Probes) were used. The human and animal studies described in this report were approved by the Ethics Review Committees of the Nagoya University Graduate School of Medicine.

Expression Plasmids, Cell Culture, and Transfection—Human wild-type SOD1 and mutant $SOD1^{G37R}$, $SOD1^{H46R}$, $SOD1^{G85R}$, and $SOD1^{G93A}$ cDNAs containing the entire coding region were inserted in-frame into the *Bam*HI and *Xho*I site of pcDNA3.1(+)/MycHis vector (Invitrogen) or into the *Xho*I and *Bam*HI site of the pEGFP-N1 vector (CLONTECH). Construction of a pcDNA3.1(+)/FLAG-Ub vector and the Dorfin or Dorfin deletion mutant (Dorfin-N and Dorfin-C) pcDNA4/HisMax vectors was reported elsewhere (14). Human embryonic kidney 293 (HEK293) cells and Neuro2a cells were maintained in Dulbecco's modified Eagle's medium with 10% fetal calf serum. Transfections were performed using the Effectene transfection reagent (Qiagen). Cells were lysed in lysis buffer (50 mM Tris, 150 mM NaCl, 1% Nonidet P-40, and 0.1% SDS) with a protease inhibitor mixture. To inhibit cellular proteasome activity, cells were treated with 0.5 μM MG132 (*N*-benzyloxycarbonyl-Leu-Leu-leucinal; Sigma) for 16 h after overnight post-transfection.

In Vitro Ubiquitylation Assay and Pulse-Chase Analysis—Immunopurified (IP) Xpress-Dorfin bound to anti-Xpress antibody (Invitrogen) with protein G beads (Amersham Biosciences) was prepared from lysates of HEK293 cells transfected with 1.5 μg of pcDNA4/HisMax-Dorfin or Dorfin deletion mutants. IP-SOD1-Myc was prepared with anti-Myc IgG-linked protein A beads (Santa Cruz Biotechnology) from lysates of HEK293 cells transfected with 1 μg of pcDNA3.1(+)MycHis wild-type or mutant SOD1. Slurries of IP-Xpress-Dorfin were mixed with IP-Myc-SOD1 and incubated at 30 °C for 90 min in 50 μl of reaction buffer containing ATP (4 mM ATP in 50 mM Tris-HCl, pH 7.5, and 2 mM $MgCl_2$), 100 ng of rabbit E1 (Calbiochem), 2 μg of UbcH7 (Affiniti, Exeter, United Kingdom), and 2 μg of His-Ub (Calbiochem). The reaction was terminated by adding 20 μl of 4× sample buffer, and 20-μl aliquots of the reaction mixtures were subjected to SDS-PAGE followed by Western blotting. Pulse-chase analysis of SOD1-transfected HEK293 cells was performed as described previously (30). Pulse labeling was performed with 250 μCi/ml [^{35}S]Cys for 45 min. After washing in phosphate-buffered saline (PBS), the cells were chased for the indicated time intervals in complete medium. Samples were immunoprecipitated with anti-Myc antibody, separated on 5–20% SDS/PAGE, and analyzed by phosphorimaging (BAS2000; Fujix, Tokyo, Japan).

Neurotoxicity Analysis and Quantification of SOD1 Aggregates—4×10^4 Neuro2a cells were grown overnight on 2-well collagen-coated slides. They were transfected with 0.4 μg of pcDNA3.1(+)/MycHis-SOD1, 0.4 μg of pcDNA4/HisMax-Dorfin, and 0.4 μg of pEGFP-C3 vector (CLONTECH). pcDNA4/HisMax-LacZ was used as control instead of Dorfin. Cells were incubated for 16 h, and the medium was then replaced with serum-free medium. Cell death was determined in propidium iodide (PI)-stained preparations at 48 h after serum deprivation. The ratio of dead cells was expressed as the percentage of PI- and GFP-positive cells in GFP-positive cells. For cell viability assay, 5×10^3 Neuro2a cells were grown in 96-well collagen-coated plates overnight. They were then transfected with 0.1 μg of pcDNA3.1(+)/MycHis-SOD1 and 0.1 μg of pcDNA4/HisMax-Dorfin. pcDNA4/HisMax-LacZ was used as control instead of Dorfin. The 3-(4,5-dimethylthiazol-2yl)-2,5-diphenyltetrazolium bromide (MTT)-based cell proliferation assay was then performed using CellTiter 96 (Promega) at 0, 24, and 48 h after incubation. The assay was carried out in triplicate. Absorbance at 490 nm was measured in a multiple plate reader. For quantification of SOD1 aggregates, Neuro2a cells transfected with pEGFP-N1-SOD1 and pcDNA4/HisMax-Dorfin or -LacZ were examined using a confocal microscope (Radiance; Bio-Rad). All cells were counted in fields selected at random from four different quadrants of the culture well. Counting was performed by an investigator blind to the experimental condition.

RESULTS

Dorfin Is Localized in the Inclusion Bodies in ALS Motor Neuron—Immunohistochemical analysis revealed that Dorfin was predominantly localized in the NHI found in familial ALS (Fig. 1, *A–C*) and mutant $SOD1^{G93A}$-transgenic mice (Fig. 1*D*) as well as in sporadic ALS (Fig. 1*E*). About 50% of NHIs were positively stained for Dorfin. Dorfin immunoreactivity was concentrated either at the periphery of the inclusion (Fig. 1*A*) or throughout it (Fig. 1*B*). Some aggregates localized in neuronal processes (Fig. 1*C*). Furthermore, Dorfin colocalized not only with SOD1-positive inclusions (Fig. 1, *F–I*) but also with Ub in NHI in both familial (Fig. 1, *J–L*) and sporadic (Fig. 1, *M–O*) ALS. Neither neural tissues not affected in ALS nor tissues other than central nervous tissue were stained with Dorfin. Only weak staining of Dorfin was diffusely observed throughout motor neurons in normal human spinal cords without neu-

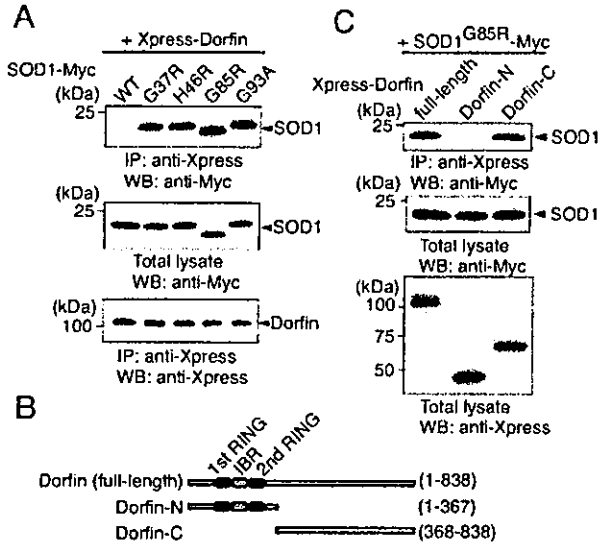

FIG. 2. **Association of Dorfin with mutant SOD1 but not wild-type SOD1 in HEK293 cells.** *A*, various Myc-tagged mutant SOD1s as indicated were co-transfected with Xpress-tagged Dorfin. After immunoprecipitation was performed with anti-Xpress antibody, the resulting precipitates and the cell lysate were analyzed by Western blotting with anti-Myc-HRP or anti-Xpress-HRP antibodies. *Arrowheads* on the *right* indicate the position of SOD1 or Dorfin. *B*, schematic representation of Dorfin and deletional mutants of Dorfin (*i.e.* Dorfin-N and Dorfin-C) used in this study. RING and IBR domains were schematically represented. *C*, binding of mutant SOD1 to the C-terminal portion of Dorfin. After Myc-tagged mutant-SOD1^{G85R} and Xpress-tagged full-length Dorfin or Dorfin-mutants were transfected, immunoprecipitation and Western blotting were performed as described in *A*.

rologic disease and non-transgenic littermate mice (data not shown). These findings suggest that Dorfin is involved in inclusion body formation via the ubiquitylation of substrate(s) yet to be identified in NHI and that SOD1 is a plausible target for ubiquitylation by Dorfin in familial ALS.

Dorfin Interacts with Mutant SOD1 but Not Wild-type SOD1—We examined whether Dorfin interacts with SOD1 *in vivo*. To this end, Xpress-tagged Dorfin was coexpressed with C-terminal Myc-tagged wild-type or various mutant forms of SOD1 in HEK293 cells. Western blotting analysis revealed that Dorfin co-immunoprecipitated with all mutant SOD1s examined here but not with wild-type SOD1 (Fig. 2*A*). However, Dorfin failed to bind either of the androgen receptors with normal (Q24) and extended (Q97) polyglutamine tracts or wild-type and mutant (A30P,A53T) α-synuclein (data not shown). Dorfin has a unique primary structure containing a RING finger/IBR motif at its N terminus and can be structurally divided into two parts, *i.e.* the N-terminal region containing a RING finger/IBR motif (Dorfin-N) that interacts with E2 and the C-terminal region with no similarity to any other known proteins (Dorfin-C) (Fig. 2*B*). We found that Dorfin-C but not Dorfin-N specifically bound mutant SOD1^{G85R} (Fig. 2*C*), indicating that Dorfin binds to the mutant SOD1 via its C-terminal region.

Dorfin Ubiquitylates Mutant SOD1 in Vitro and Promotes Ubiquitylation and Degradation of SOD1 in Vivo—Physical interaction between Dorfin and mutant SOD1 prompted us to investigate whether SOD1 itself is ubiquitylated by Dorfin. We first examined whether SOD1 is ubiquitylated in a culture cell model. C-terminal Myc-tagged wild-type or mutant SOD1 was co-transfected with FLAG-tagged Ub in HEK293 cells. When SOD1 was immunoprecipitated after treatment with the proteasome inhibitor MG132, all mutant SOD1s, unlike wild-type SOD1, were found to be polyubiquitylated (Fig. 3*A*). In addition, ectopic expression of Dorfin increased the ubiquitylation of mutant SOD1^{G85R} without affecting the wild-type SOD1 (Fig. 3*B*).

We next examined whether Dorfin directly ubiquitylates SOD1 *in vitro*. For this purpose, we prepared IP Xpress-Dorfin or its deletion mutants and IP wild-type or mutant SOD1^{G85R}-Myc without proteasome inhibitor after transfection into HEK293 cells, independently. When these immunoprecipitates were incubated with recombinant E1, E2 (UbcH7), His-tagged Ub, and ATP, high molecular weight ubiquitylated bands were observed in the presence of IP-Xpress-Dorfin with mutant SOD1^{G85R}, whereas no signal was noted in wild-type SOD1 or mutant SOD1^{G85R} in the absence of either Dorfin, E1, or E2 (Fig. 3*C*). Deletion mutants of Dorfin (Dorfin-N or Dorfin-C) did not show a significant activity upon ubiquitylation against mutant SOD1^{G85R} (Fig. 3*C*), indicating that both E2-recruiting N-terminal and substrate-binding C-terminal portions are required for Dorfin–mediated ubiquitylation. Further *in vitro* studies using other mutants showed that Dorfin also ubiquitylated SOD1^{G37R} and SOD1^{G93A} significantly and ubiquitylated SOD1^{H46R} as well, although to a lesser extent (Fig. 3*D*).

Mutant SOD1 protein has a short half-life compared with wild-type SOD1 as shown previously by pulse-chase experiments (30, 32, 33). By blocking the ubiquitin-proteasome pathway, its half-life can be elongated (30, 33). We examined whether the *in vivo* stability of wild-type and mutant SOD1 is affected by Dorfin. We used pulse-chase analysis to evaluate the stability of wild-type and mutant Myc-tagged SOD1 expressed in HEK293 cells in the presence or absence of Dorfin. Pulse-chase experiments revealed that ^{35}S-labeled SOD1^{G85R} was fairly unstable compared with its wild-type version, and the degradation of SOD1^{G85R} was greatly accelerated when Dorfin was overexpressed, whereas the stability of wild-type SOD1 was unaffected (Fig. 3*E*).

Dorfin Protects Neuronal Cells from Mutant SOD1-mediated Neurotoxicity through Its E3 Activity and Reduces SOD1 Inclusion Bodies—Based on these observations, we inferred that Dorfin protects cells against mutant SOD1-mediated neurotoxicity. To study neuronal cell death induced by mutations in SOD1, we used a mouse neuroblastoma cell line (Neuro2a) transiently transfected with wild-type and a mutant (G85R and G93A). These cells are maintained as nondifferentiated dividing cells but can be induced to differentiate to be neural cells by serum deprivation (34). We transfected SOD1 with Dorfin or LacZ into Neuro2a cells and induced neural differentiation by serum deprivation after overnight post-transfection. Co-expression of Dorfin significantly reduced the percentages of PI-positive dead cells in both mutant SOD1^{G85R}- and SOD1^{G93A}-transfected cells compared with those in cells co-expressing LacZ (Fig. 4*A*). In contrast, Dorfin-N and Dorfin-C had no protective activity, indicating that the E3 activity of Dorfin is essential for the suppression of mutant SOD1-induced neuronal cell death. We also found a similar Dorfin-dependent protective effect against the loss of neuronal cell viability evoked by mutant SOD1 using the MTT assay (Fig. 4*B*). One hypothesis argues that toxicity results from the tendency of mutant SOD1 to aggregate into the cytoplasmic inclusion bodies (35) that are evident in cultured spinal motor neurons (36) and COS7 cells (37) expressing mutant SOD1 cDNA or in motor neurons from SOD1 transgenic mice (38, 39). In our experimental model, the expression of mutant SOD1^{G85R} induced perinuclear intracytoplasmic inclusion bodies in Neuro2a cells (Fig. 4*C*, *left panel*). The overexpression of Dorfin significantly reduced the number of aggregates in SOD1^{G85R}-transfected Neuro2a cells (Fig. 4*C*, *right panel*, and 4*D*).

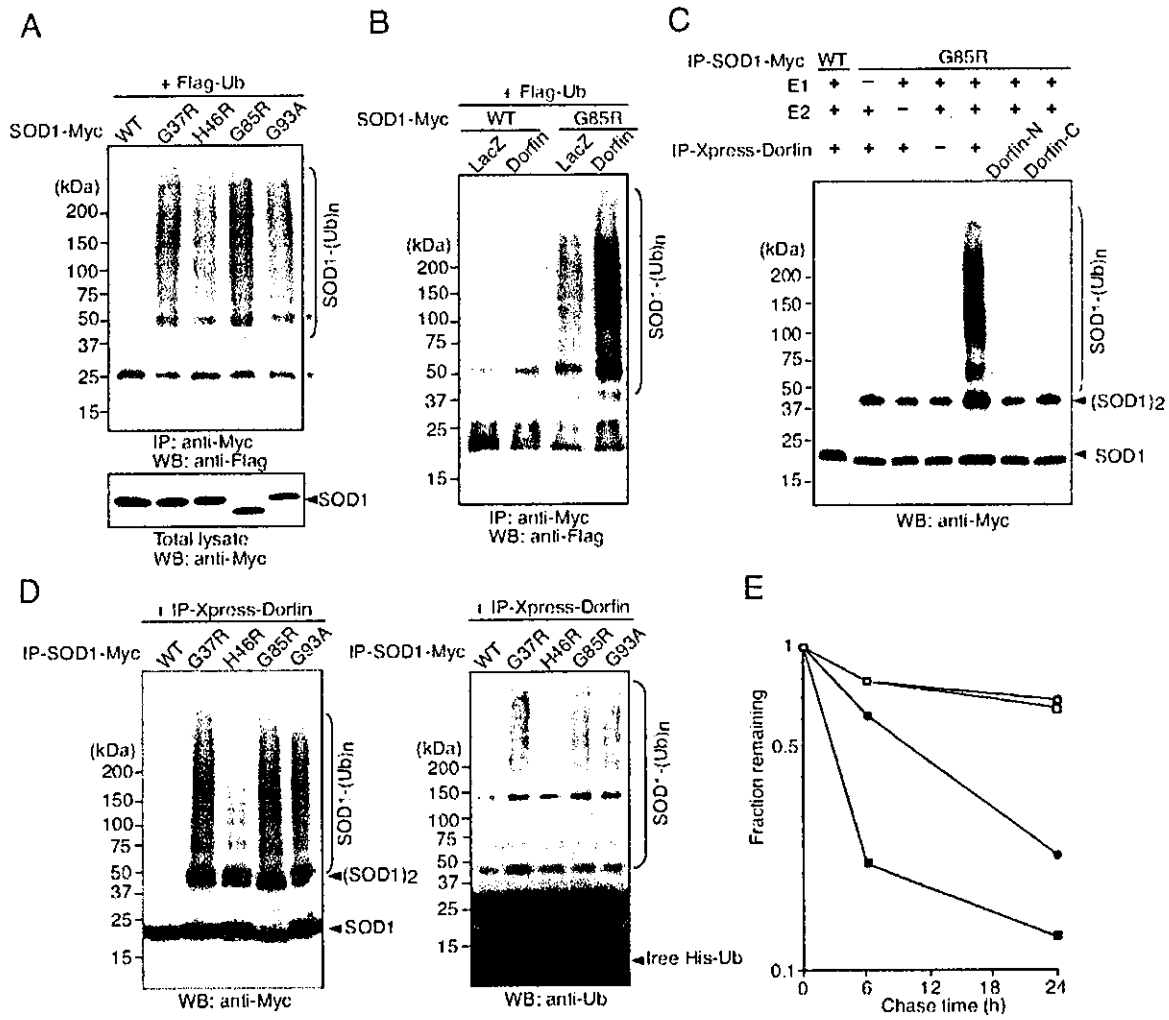

FIG. 3. **Ubiquitylation of mutant SOD1 by Dorfin.** *A*, mutant SOD1s were ubiquitylated in HEK293 cells, which were co-transfected with Myc-tagged wild-type SOD1 or SOD1 mutants (as indicated) and FLAG-tagged Ub. These cells were treated with 0.5 μM MG132 for 16 h after overnight post-transfection. Immunoprecipitates prepared by an anti-Myc antibody were used for immunoblotting with the anti-FLAG antibody. The high molecular-mass ubiquitylated SOD1s are shown as SOD1-(Ub)n on the *right* (*upper panel*). *Asterisks* indicate IgG light and heavy chains. The blot shown is a representative blot from three independent experiments. Total lysate was used for Western blot with the anti-Myc antibody (*lower panel*). *Asterisk* on the *right* indicates the position of SOD1. *B*, increased ubiquitylation of SOD1^{G85R} by overexpression of Dorfin. HEK293 cells were co-transfected with Myc-tagged wild-type SOD1 or SOD1^{G85R} mutants and FLAG-tagged Ub in the presence of Dorfin or LacZ. Immunoprecipitation and immunoblotting were performed as described in *A*. *C*, *in vitro* ubiquitylation assay of SOD1^{G85R} by Dorfin. Xpress-tagged Dorfin and Myc-tagged SOD1 were transfected into HEK293 cells independently. Immunoprecipitated Dorfin (IP Xpress-Dorfin) and SOD1 (IP-SOD1-Myc) were prepared and mixed in an assay mixture for ubiquitylation. For this assay, wild-type and mutant SOD1^{G85R} and full-length Dorfin, Dorfin-N, and Dorfin-C were used. After a 90-min incubation at 30 °C, SDS-PAGE was performed followed by Western blotting for SOD1 with the anti-Myc antibody. Monomeric, dimeric, and the high molecular mass-ubiquitylated SOD1 are shown on the *right*. Note that only mutant SOD1 showed SDS-resistant dimeric banding indicated by *(SOD1)2*. *D*, *in vitro* ubiquitylation assay of various SOD1 mutants by Dorfin. The ubiquitylation assay was carried out as described in *C* except that various SOD1 mutants were used as indicated, and Western blotting was also conducted with an anti-Myc antibody (*left panel*) for the detection of SOD1 as well as anti-Ub antibody (*right panel*). *E*, accelerated degradation of mutant SOD1^{G85R} by Dorfin. HEK293 cells transiently expressing wild-type (*open circles* and *open squares*) or mutant SOD1^{G85R} (*closed circles* and *closed squares*) were pulse-labeled with [^{35}S]Cys for 45 min and chased for the time intervals indicated under the overexpression of Dorfin (*open squares* and *closed squares*) or LacZ (*open circles* and *closed squares*). Data are mean values of three independent experiments.

DISCUSSION

In the present study, we showed for the first time that mutant SOD1s are selectively degraded through a Dorfin-mediated Ub-proteasome pathway and that Dorfin protects neuronal cells against the toxic effects of mutant SOD1. Whereas Dorfin can ubiquitylate mutant SOD1s, probably because of their fragile or misfolded conformation, the constant production of high amounts of impaired SOD1 in familial ALS becomes a burden on the protein degradation process through the Ub-proteasome pathway, eventually overwhelming the capacity of the proteasome to degrade toxic SOD1 and subsequently leading to the accumulation of ubiquitylated SOD1 and motor neuron death. Consistent with this scenario, recent studies reported that impairment of the Ub-proteasome system is caused by protein aggregation (40). Thus, up-regulation or exogenous expression of Dorfin may be therapeutically beneficial in familial ALS. Our results also showed that Dorfin colocalized with ubiquitylated inclusions not only in familial ALS but also in sporadic ALS. Based on this finding, it is conceivable that familial and sporadic forms of ALS share a common mechanism

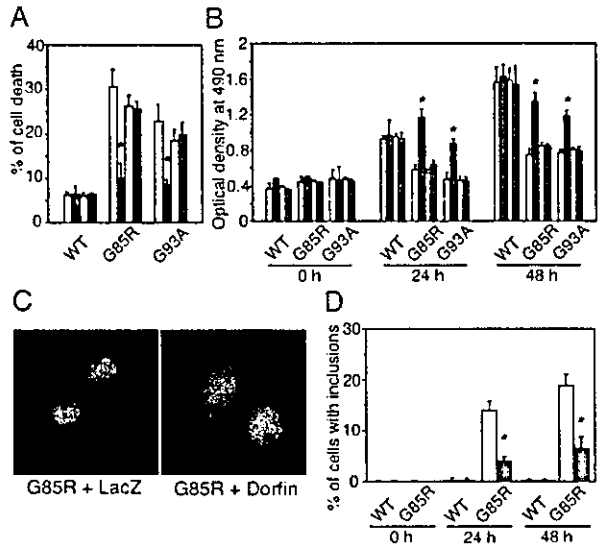

FIG. 4. **Dorfin protects neural cells against mutant SOD1-mediated toxicity.** *A*, cell death assay using PI staining. Neuro2a cells were grown on collagen-coated 2-chamber well slides and transfected with Myc-tagged SOD1 (wild-type, $SOD1^{G86R}$, and $SOD1^{G93A}$) and Xpress-tagged Dorfin (full-length, *red bars*; Dorfin-N, *yellow bars*; Dorfin-C, *green bars*). Xpress-tagged LacZ (*white bars*) was used as control. The pEGFP-C3 vector was also transfected as a marker of transfected cells. After 48 h of serum withdrawal, the proportions of PI- and GFP-positive cells among the GFP-positive cells were counted. Data are mean ± S.D. values of triplicate assays. Statistical analyses were carried out by one-way analysis of variance (ANOVA). *, $p < 0.001$. *B*, the rescue effect of Dorfin expression in mutant SOD1-transfected cells on an MTT assay. Neuro2a cells were grown on collagen-coated 96-well plates and transfected as described in *A*. After changing the medium to serum-free, MTT assays were performed after 0, 24, and 48 h of incubation. Viability was measured as the level of absorbance at 490 nm. Data are mean ± S.D. values of triplicate assays. Statistical analyses were carried out by one-way ANOVA. *, $p < 0.001$. *C* and *D*, the reduction of mutant SOD1 aggregates by Dorfin. Neuro2a cells grown on collagen-coated 2-chamber well slides were transfected with a GFP-tagged wild type or mutant $SOD1^{G85R}$ in the presence of Dorfin (*red bars*) or LacZ (*white bars*). After 48 h of serum withdrawal, slides were examined using a laser-scanning confocal microscope. *Panel C* shows a typical example in which the overexpression of Dorfin reduces $SOD1^{G85R}$ aggregate-bearing Neuro2a cells. The percentages of aggregate-positive cells among the GFP-positive cells were determined in *D*. Data are the mean ± S.D. values of triplicate assays. Statistical analyses were carried out by Mann-Whitney's *U* test. *, $p < 0.01$.

involving the dysfunction of the Ub-proteasome pathway despite distinct etiological mechanisms.

Studies of parkin have provided new insights into the importance of the ubiquitin-proteasome pathway in the neuronal degeneration of PD. Parkin was shown to have E3 activity (19–21). Recently, an *O*-glycosylated form of α-synuclein and synphilin-1 were shown to be substrates of parkin (41, 42). Both α-synuclein and synphilin-1 are major components of Lewy bodies, which are ubiquitylated inclusion bodies characteristic of sporadic PD. A link between sporadic and familial PD through α-synuclein, synphilin-1, and parkin suggests that common molecular pathogenic mechanisms underlie PD. The accumulation of toxic or undesired proteins in neurons may result from the failure of degradation systems and could subsequently lead to neurodegeneration. From this point of view, in sporadic ALS post-translationally modified SOD1 (43) or other unknown substrates might accumulate in the ubiquitylated form and play a role in the pathogenesis of the disease.

Our results raise an important question related to the function of Dorfin; what is the biological role of Dorfin and how does Dorfin recognize the abnormal mutant SOD1? Because we used IP-Dorfin and IP-mutant SOD1 for an ubiquitylating assay here, it is possible that Dorfin interacts with mutant SOD1 indirectly. Recently CHIP (carboxyl terminus of Hsc70-interacting protein), an U-box type E3, has been shown to interact with Hsp90 or Hsp70 and ubiquitylate unfolded proteins captured by these molecular chaperones in a selective manner, thus acting as a "quality control E3" (44, 45). Likewise, because Dorfin can discriminate between the normal and abnormal status of SOD1 proteins, it can be regarded as another quality control E3. However, preliminary results showed that CHIP did not ubiquitylate mutant SOD1s (data not shown); therefore, Dorfin possesses a distinct way for recognition of the abnormality of SOD1. It is possible that a novel sequence within the C terminus of Dorfin may associate with a substrate-recognizing molecule(s) (corresponding to Hsp in CHIP) or facilitate a unique mechanism for trapping the target in a direct or indirect manner. Further studies should be designed to determine this mechanism, which should enhance our understanding of Dorfin function *in vivo* and its relationship to ALS pathogenesis.

Acknowledgment—We thank Dr. J. Q. Trojanowski for helpful comments.

REFERENCES

1. Tyler, H. R., and Shefner, J. (1991) in *Handbook of Clinical Neurology* (Vinken P. J., Bruyn, G. W., and Klawans, H. L., eds) Vol. 59, pp. 169–215, Elsevier Science Publishers B. V., Amsterdam
2. Emery, A., and Holloway, S. (1982) in *Human Motor Neuron Diseases* (Rowland, L., ed), pp. 139–147, Raven Press, Ltd., New York
3. Rosen, D. R., Siddique, T., Patterson, D., Figlewicz, D. A., Sapp, P., Hentati, A., Donaldson, D., Goto, J., O'Regan, J. P., Deng, H. X., Rahmani, Z., Krizus, A., McKenna-Yasek, D., Cayabyab, A., Gaston, S. M., Berger, R., Tanzi, R. E., Halperin, J. J., Herzfeldt, B., Van den Bergh, R., Hung, W.-Y., Bird, T., Deng, G., Mulder, D. W., Smyth, C., Laing, N. G., Soriano, E., Pericak-Vance, M. A., Haines, J., Rouleau, G. A., Gusella, J. S., Horvitz, H. R., and Brown, R. H., Jr. (1993) *Nature* **362**, 59–62
4. Julien, J. P. (2001) *Cell* **104**, 581–591
5. Cleveland, D. W., and Rothstein, J. D. (2001) *Nat. Rev. Neurosci.* **2**, 806–819
6. Newbery, H. J., and Abbott, C. M. (2002) *Trends Mol. Med.* **8**, 88–92
7. Hirano, A. (1996) *Neurology* **47**, S63–S66
8. Murayama, S., Mori, H., Ihara, Y., Bouldin, T. W., Suzuki, K., and Tomonaga, M. (1990) *Ann. Neurol.* **27**, 137–148
9. Leigh, P. N., Whitwell, H., Garofalo, O., Buller, J., Swash, M., Martin, J. E., Gallo, J. M., Weller, R. O., and Anderton, B. H. (1991) *Brain* **114**, 775–788
10. Schiffer, D., Autilio-Gambetti, L., Chio, A., Gambetti, P., Giordana, M. T., Gullotta, F., Migheli, A., and Vigliani, M. C. (1991) *J. Neuropathol. Exp. Neurol.* **50**, 463–473
11. Lowe, J. (1994) *J. Neurol. Sci.* **124**, S38–S51
12. Kato, S., Takikawa, M., Nakashima, K., Hirano, A., Cleveland, D. W., Kusaka, H., Shibata, N., Kato, M., Nakano, I., and Ohama, E. (2000) *Amyotroph. Lateral Scler. Other Motor Neuron Disord.* **1**, 163–184
13. Shibata, N., Hirano, A., Kobayashi, M., Siddique, T., Deng, H. X., Hung, W. Y., Kato, T., and Asayama, K. (1996) *J. Neuropathol. Exp. Neurol.* **55**, 481–490
14. Niwa, J., Ishigaki, S., Doyu, M., Suzuki, T., Tanaka, K., and Sobue, G. (2001) *Biochem. Biophys. Res. Commun.* **281**, 706–713
15. Morett, E., and Bork, P. (1999) *Trends Biochem. Sci.* **24**, 229–231
16. Moynihan, T. P., Ardley, H. C., Nuber, U., Rose, S. A., Jones, P. F., Markham, A. F., Scheffner, M., and Robinson, P. A. (1999) *J. Biol. Chem.* **274**, 30963–30968
17. Ardley, H. C., Tan, N. G., Rose, S. A., Markham, A. F., and Robinson, P. A. (2001) *J. Biol. Chem.* **276**, 19640–19647
18. Kitada, T., Asakawa, S., Hattori, N., Matsumine, H., Yamamura, Y., Minoshima, S., Yokochi, M., Mizuno, Y., and Shimizu, N. (1998) *Nature* **392**, 605–608
19. Shimura, H., Hattori, N., Kubo, S., Mizuno, Y., Asakawa, S., Minoshima, S., Shimizu, N., Iwai, K., Chiba, T., Tanaka, K., and Suzuki, T. (2000) *Nat. Genet.* **25**, 302–305
20. Imai, Y., Soda, M., and Takahashi, R. (2000) *J. Biol. Chem.* **275**, 35661–35664
21. Zhang, Y., Gao, J., Chung, K. K., Huang, H., Dawson, V. L., and Dawson, T. M. (2000) *Proc. Natl. Acad. Sci. U. S. A.* **97**, 13354–13359
22. Joazeiro, C. A., Wing, S. S., Huang, H., Leverson, J. D., Hunter, T., and Liu, Y. C. (1999) *Science* **286**, 309–312
23. Lorick, K. L., Jensen, J. P., Fang, S., Ong, A. M., Hatakeyama, S., and Weissman, A. M. (1999) *Proc. Natl. Acad. Sci. U. S. A.* **96**, 11364–11369
24. Yang, Y., Fang, S., Jensen, J. P., Weissman, A. M., and Ashwell, J. D. (2000) *Science* **288**, 874–877
25. Freemont, P. S. (2000) *Curr. Biol.* **10**, R84–R87
26. Deshaies, R. J. (1999) *Annu. Rev. Cell Dev. Biol.* **15**, 435–467
27. Joazeiro, C. A., and Weissman, A. M. (2000) *Cell* **102**, 549–552
28. Jackson, P. K., Eldridge, A. G., Freed, E., Furstenthal, L., Hsu, J. Y., Kaiser, B. K., and Reimann, J. D. R. (2000) *Trends Cell Biol.* **10**, 429–439
29. Johnston, J. A., Ward, C. L., and Kopito, R. R. (1998) *J. Cell Biol.* **143**, 1883–1898
30. Johnston, J. A., Dalton, M. J., Gurney, M. E., and Kopito, R. R. (2000) *Proc.*

Natl. Acad. Sci. U. S. A. **97,** 12571–12576
31. Hishikawa, N., Hashizume, Y., Yoshida, M., and Sobue G. (2001) *Neuropathol. Appl. Neurobiol.* **27,** 362–372
32. Borchelt, D. R., Lee, M. K., Slunt, H. S., Guarnieri, M., Xu, Z. S., Wong, P. C., Brown, R. H., Jr., Price, D. L., Sisodia, S. S., and Cleveland, D. W. (1994) *Proc. Natl. Acad. Sci. U. S. A.* **91,** 8292–8296
33. Hoffman, E. K., Wilcox, H. M., Scott, R. W., and Siman, R. (1996) *J. Neurol. Sci.* **139,** 15–20
34. Pasinelli, P., Borchelt, D. R., Houseweart, M. K., Cleveland, D. W., and Brown, R. H., Jr. (1998) *Proc. Natl. Acad. Sci. U. S. A.* **95,** 15763–15768
35. Bruijn, L. I., Houseweart, M. K., Kato, S., Anderson, K. L., Anderson, S. D., Ohama, E., Reaume, A. G., Scott, R. W., and Cleveland, D. W. (1998) *Science* **281,** 1851–1854
36. Durham, H. D., Roy, J., Dong, L., and Figlewicz D. A. (1997) *J. Neuropathol. Exp. Neurol.* **56,** 523–530
37. Koide, T., Igarashi, S., Kikugawa, K., Nakano, R., Inuzuka, T., Yamada, M., Takahashi, H., and Tsuji, S. (1998) *Neurosci. Lett.* **257,** 29–32
38. Tu, P. H., Raju, P., Robinson, K. A., Gurney, M. E., Trojanowski, J. Q., and Lee, V. M. (1996) *Proc. Natl. Acad. Sci. U. S. A.* **93,** 3155–3160
39. Bruijn, L. I., Becher, M. W., Lee, M. K., Anderson, K. L., Jenkins, N. A., Copeland, N. G., Sisodia, S. S., Rothstein, J. D., Borchelt, D. R., Price, D. L., and Cleveland, D. W. (1997) *Neuron* **18,** 327–338
40. Bence, N. F., Sampat, R. M., and Kopito, R. R. (2001) *Science* **292,** 1552–1555
41. Shimura, H., Schlossmacher, M. G., Hattori, N., Frosch, M. P., Trockenbacher, A., Schneider, R., Mizuno, Y., Kosik, K. S., and Selkoe, D. J. (2001) *Science* **293,** 263–269
42. Chung, K. K., Zhang, Y., Lim, K. L., Tanaka, Y., Huang, H., Gao, J., Ross, C. A., Dawson, V. L., and Dawson, T. M. (2001) *Nat. Med.* **7,** 1144–1150
43. Bredesen, D. E., Ellerby, L. M., Hart, P. J., Wiedau-Pazos, M., and Valentine, J. S. (1997) *Ann. Neurol.* **42,** 135–137
44. McClellan, A. J., and Frydman, J. (2001) *Nat. Cell. Biol.* **3,** E51–E53
45. Murata, S., Minami, Y., Minami, M., Chiba, T., and Tanaka, K. (2001) *EMBO Rep.* **2,** 1133–1138

ELSEVIER

Brain Research 949 (2002) 11–22

BRAIN RESEARCH

www.elsevier.com/locate/bres

Research report

Hsp70 and Hsp40 improve neurite outgrowth and suppress intracytoplasmic aggregate formation in cultured neuronal cells expressing mutant SOD1

Hideyuki Takeuchi[a], Yasushi Kobayashi[a], Tsuyoshi Yoshihara[a], Jun-ichi Niwa[a], Manabu Doyu[a], Kenzo Ohtsuka[b], Gen Sobue[a,*]

[a]*Department of Neurology, Nagoya University Graduate School of Medicine, 65 Tsurumai-cho, Showa-ku, Nagoya 466-8550, Japan*
[b]*Laboratory of Cell and Stress Biology, College of Bioscience and Biotechnology, Chubu University, 1200 Matsumoto-cho, Kasugai, Aichi 487-8501, Japan*

Accepted 19 December 2001

Abstract

Mutations of the superoxide dismutase 1 (SOD1) gene cause familial amyotrophic lateral sclerosis (FALS). Intracytoplasmic aggregate formation consisting of mutant SOD1 is the histological hallmark of FALS. Since a previous report revealed that Hsp70 reduced aggregate formation and cell death in a cell model of FALS, here we examined the combined effects of Hsp70 and its cofactor, Hsp40, on a cell model of FALS. The combination of Hsp70 and Hsp40 reduced intracytoplasmic aggregates and markedly improved neurite outgrowth. They also prevented cell death to a relatively lesser extent. Neurite outgrowth was recognized almost exclusively in the cells without intracytoplasmic aggregates. Hsp70 and Hsp40 were upregulated in cells expressing mutant SOD1, and were colocalized with intracytoplasmic aggregates of mutant SOD1. These findings suggest that heat shock proteins (HSPs) promote neurite outgrowth by suppressing intracytoplasmic aggregate formation and restoring cellular dysfunctions. This is the first demonstration that overexpression of HSPs improved neurite outgrowth as it suppressed intracytoplasmic aggregate formation and cell death in a cultured neuronal cell model of FALS. These findings may provide a basis for the utilization of HSPs in developing a treatment for FALS.

Theme: Disorders of the nervous system

Topic: Degenerative disease: other

Keywords: Familial amyotrophic lateral sclerosis; Superoxide dismutase 1; Heat shock protein; Neuro2a; Intracytoplasmic aggregate; Neurite outgrowth; Cell death

1. Introduction

Familial amyotrophic lateral sclerosis (FALS), an autosomal dominant inherited form of ALS, is a progressive and lethal motor neuron disease. The intracytoplasmic aggregate formation, which is called Lewy body-like hyaline inclusion, is a characteristic pathological feature of FALS [18,19]. Mutations of superoxide dismutase 1 (SOD1) have been found as a cause of 15 to 20% of FALS cases [36], and mutant SOD1 has been suggested to have a gain of a new and toxic function that is involved in the pathogenic mechanism of FALS with SOD1 [50]. The intracytoplasmic aggregate formation of mutant SOD1 is thought to be one of the toxic factors leading to neuronal cell death [4,12]. Intracytoplasmic mutant SOD1 aggregates were recently suggested to be a product processed by the retrograde transport on microtubules forming an aggresome [22], where the ubiquitin–proteasome proteolytic pathway plays a role in disposing of abnormal proteins [5,25,39]. Heat shock proteins (HSPs) function as molecular chaperones that recognize and renaturate misfolded proteins and maintain proteins in an appropriate conformation [14,17,30,31,33]. We previously demonstrated that HSPs, especially the combination of Hsp70 and Hsp40,

*Corresponding author. Tel.: +81-52-744-2385; fax: +81-52-744-2384.
E-mail address: sobueg@med.nagoya-u.ac.jp (G. Sobue).

0006-8993/02/$ – see front matter
PII: S0006-8993(02)02568-4

suppressed intranuclear aggregate formation and cell death in a cultured neuronal cell model of spinal and bulbar muscular atrophy, a polyglutamine disease [23]. A similar protective effect of HSPs has been documented in the in vitro and in vivo models of a wide range of polyglutamine diseases [7,8,10,46]. In a motor neuron culture model of the FALS expressing mutant Gly93Ala (G93A) SOD1, microinjection of Hsp70 also showed the effects on aggregate suppression and cell survival [3]. Since the Hsp70 and Hsp40 chaperone family members act together to promote cellular protein folding and renaturate misfolded proteins [8,14,17,30,31,33], the combined overexpression of Hsp70 and Hsp40 chaperones could facilitate the refolding and proteolysis of the mutant protein, and could defend the neuronal cells against the toxic properties of mutant SOD1.

In the present study, we demonstrated that overexpression of HSPs, especially the combination of Hsp70 and Hsp40, suppressed intracytoplasmic aggregate formation and improved neurite outgrowth and cell death in cultured neuronal cells expressing mutant SOD1.

2. Materials and methods

2.1. Plasmid constructs

2.1.1. Mutant and wild-type human SOD1

Baculoviral vectors containing mutant (G93A) and wild-type human SOD1 were the kind gifts of Dr. Moon Bin Yim (the Laboratory of Biochemistry, NHLBI, National Institute of Health, Bethesda, Maryland). After the constructs were digested with Sma I and blunt-ended, G93A and wild-type SOD1 were subcloned into pEGFP-N1 vector (Clontech).

2.1.2. Chaperones and mock

DNA-pCMV-Hsp70 and pCMV-Hsp40 were constructed as described previously [23,30]. pCMV-(Clontech) was used as a mock DNA. All constructs used here were confirmed by DNA sequence analysis.

2.2. Cell culture and immunofluorescence stain

Transient expression of wild-type and G93A SOD1–EGFP fusion protein (0.4 μg of DNA/well) in Neuro2a cells (20,000 cells/well) was accomplished with Effectene (Qiagen). Then in the cotransfection experiments, we also achieved transient expression of wild-type SOD1–EGFP plus mock DNA (0.2 μg+0.2 μg of DNA/well), G93A SOD1–EGFP plus mock DNA (0.2 μg+0.2 μg of DNA/well), G93A SOD1–EGFP plus Hsp70 (0.2 μg+0.2 μg of DNA/well), G93A SOD1–EGFP plus Hsp40 (0.2 μg+0.2 μg of DNA/well) and G93A SOD1–EGFP plus Hsp70 plus Hsp40 (0.2 μg+0.1 μg+0.1 μg of DNA/well) in Neuro2a cells (20,000 cells/well). They were cultured in a four-chamber slide (Nalge Nunc International) coated with rat's tail collagen (Roche Diagnostics GmbH) in Dulbecco's modified Eagle's medium (Life Technologies Inc.) supplemented with 10% fetal calf serum. After overnight incubation with transfection reagents, transfected cells were cultured in differentiation medium (Dulbecco's modified Eagle's medium supplemented with 2% fetal calf serum and 20 μM retinoic acid). At each time point (0, 24, 48 and 72 h) after transfection, cells were fixed with methanol for 10 min on ice. Rabbit polyclonal anti-Hsp70 IgG, rabbit polyclonal anti-Hsp40 IgG (1:1000, respectively, StressGen Biotechnologies Corp.), mouse monoclonal anti-vimentin IgG (1:500, Sigma) were used as the primary antibodies for immunostaining. The fixed cells were incubated with these antibodies at 4 °C overnight. They were subsequently stained with goat anti-rabbit IgG or goat anti-mouse IgG conjugated with Alexa 568 (1:1000, Molecular Probes) at room temperature for 90 min. Then they were counterstained with 2 μM TOTO-3 (Molecular Probes) at room temperature for 10 min, and mounted in Gelvatol.

2.3. Quantitative assessment of intracytoplasmic aggregates and neurite outgrowth

A laser-confocal scanning microscope (MRC1024, Bio-Rad) was used for quantitative analysis. At each time point (0, 24, 48 and 72 h) after transfection, cells were fixed with methanol for 10 min on ice, followed by counterstaining with 2.5 μg/ml propidium iodide (Molecular Probes) and mounted in Gelvatol. Over 200 transfected cells in duplicate slides were assessed blindly in three independent trials. The frequency of intracytoplasmic aggregate-containing cells was calculated as the number of such cells divided by that of EGFP-positive cells. To evaluate the frequency of neurite-bearing cells, the cells with neurites exceeding the cell diameter were counted by a modification of the method previously reported by Li et al. [27]. The frequency was also calculated as the number of both EGFP-positive and neurite-bearing cells divided by that of total EGFP-positive cells. Then we assessed the frequency of neurite-bearing cells among intracytoplasmic aggregate-containing cells or aggregate-negative (but EGFP-positive) cells. Over 200 intracytoplasmic aggregate-containing cells or aggregate-negative (but EGFP-positive) cells in duplicate slides were assessed blindly in three independent trials 48 h after transfection. The frequency was calculated as the number of neurite-bearing cells divided by that of intracytoplasmic aggregate-containing cells or aggregate-negative (but EGFP-positive) cells.

2.4. Quantitative assessment of cell death

Cell death was assessed by propidium iodide staining

and cytotoxic assay using luciferase assay. At each time point (0, 24, 48 and 72 h) after transfection, cells were incubated with 2 μg/ml propidium iodide (Molecular Probes) for 15 min at room temperature and mounted in Gelvatol. Over 200 transfected cells in duplicate slides were assessed blindly in three independent trials under a conventional fluorescent microscope.

The frequency of dead cells was calculated as the number of both EGFP-positive and propidium iodide-positive cells divided by that of total EGFP-positive cells. For cytotoxic assay, we used a luciferase assay kit (Promega) according to the method previously described [11,20,48]. The Neuro2a cells (500,000 cells/60 mm-culture dish) were transfected with the pGL3 luciferase reporter vector in one-tenth the amount of total DNA. Each assay carried out in duplicate was repeated three times. At each time point (0, 24, 48, and 72 h) after transfection, luciferase activity was measured by luminometry and normalized by the protein concentration determined with a DC protein assay kit (Bio-Rad).

2.5. Western blots

At each time point (12, 24, 48, and 72 h) after transfection, cells were lysed in RIPA buffer (50 mM Tris, 150 mM NaCl, 1% NP-40, 0.1% sodium dodecyl sulfate, and 10 μg/ml aprotinin). Insoluble debris was pelleted, and the protein concentration of the supernatant was determined with a DC protein assay kit (Bio-Rad). A 20-μg sample was electrophoresed on a standard sodium dodecyl sulfate–polyacrylamide gel and transferred to Hybond-P (Amersham Pharmacia Biotech). Blots were probed with the indicated antibodies using rabbit polyclonal anti-SOD1 IgG, rabbit polyclonal anti-Hsp70 IgG, and rabbit polyclonal anti-Hsp40 IgG (1:5000 respectively, StressGen Biotechnologies Corp.) coupled to horseradish

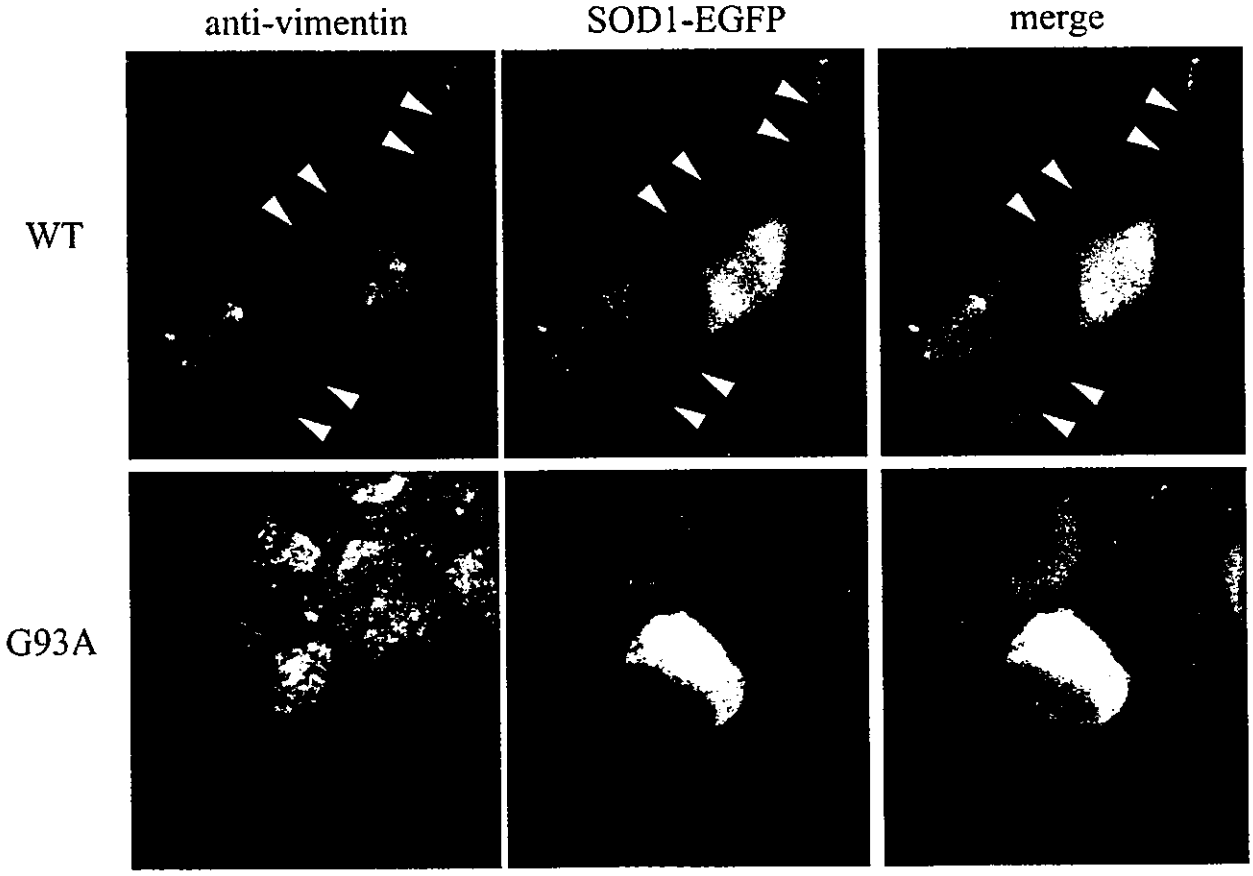

Fig. 1. Overexpression of mutant SOD1 induced intracytoplasmic aggregate formation and inhibition of neurite outgrowth. Overlays of three images were taken by laser confocal microscopy 48 h after transfection. The cell shape was clearly depicted by immunofluorescent staining with vimentin (red), and fluorescence of SOD1–EGFP (green). Wild-type SOD1-transfected cells showed SOD1–EGFP fusion protein diffusely throughout the cytoplasm and neurite outgrowth (arrowheads). By contrast, mutant SOD1-transfected cells showed intracytoplasmic aggregate formation containing SOD1–EGFP fusion protein and blast-like morphology with few neurites. The nucleus was stained with TOTO-3 (blue). WT, wild-type SOD1; G93A, mutant G93A SOD1.

peroxidase-conjugated anti-rabbit IgG (Amersham Pharmacia Biotech). Then they were developed with enhanced chemiluminescence reagents (Amersham Pharmacia Biotech). At least six independent Western blots were carried out and the signal intensity was quantified by densitometry. The relative signal intensity (RSI) of SOD1–EGFP was calculated as the signal intensity of the indicated band divided by that of an endogenous SOD1 band in the same lane. The RSI of HSPs was also calculated as the signal intensity of the indicated band divided by that of the band with non-transfected cells.

2.6. Statistical analysis

Results were analyzed by analysis of variance and Student's *t*-test using Statview software version 5 (SAS Institute Inc.).

3. Results

3.1. Cells with aggregate formation of mutant SOD1 demonstrate inhibition of neurite outgrowth as well as cell death

Transient expression of mutant G93A SOD1 induced an intracytoplasmic aggregate formation (Figs. 1, 2B and 3A), a blast-like morphology with few neurites (Figs. 1, 2B and 3B), and cell death (Fig. 3C and D). Expression of wild-type SOD1 induced neither aggregate formation, inhibition of neurite outgrowth, nor cell death (Figs. 1, 2A and 3). Transient expression of the empty vector alone showed results similar to those of wild-type SOD1 (data not shown). Frequency of cells containing aggregates peaked 48 h after mutant SOD1 transfection (Fig. 3A). Frequency of neurite outgrowth was consistently much lower in the

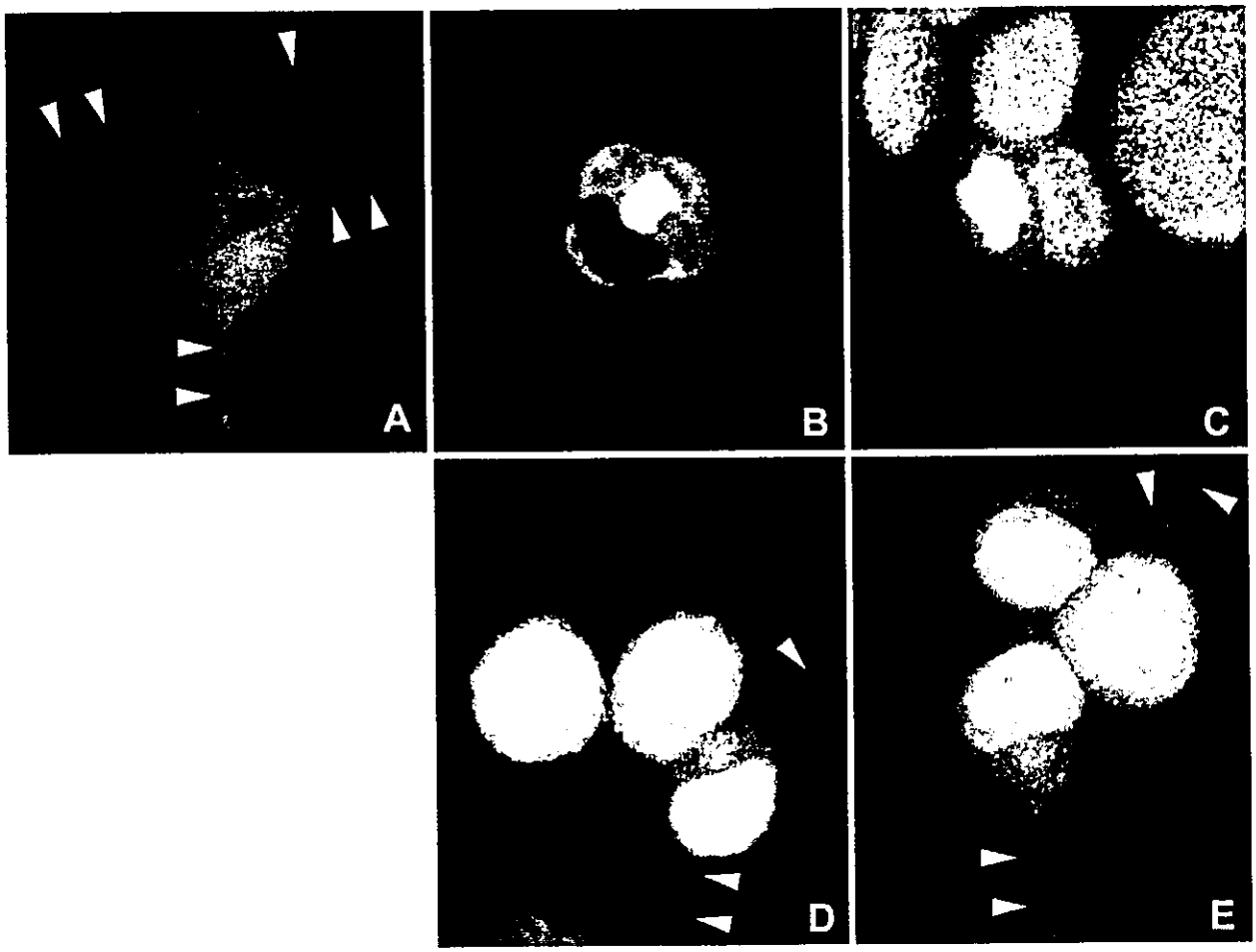

Fig. 2. HSPs suppress intracytoplasmic aggregate formation and ameliorate neurite outgrowth. Overlays of two images were taken by laser-confocal microscopy 48 h after transfection. (A) Wild-type SOD1-transfected cells showed SOD1–EGFP fusion protein diffusely throughout the cytoplasm (green) and neurite outgrowth (arrowheads). (B) By contrast, G93A SOD1-transfected cells showed intracytoplasmic aggregates containing SOD1–EGFP fusion protein and few neurites. (C) Cotransfected with mutant G93A SOD1 and Hsp40. (D) Cotransfected with mutant G93A SOD1 and Hsp70. (E) Cotransfected with mutant G93A SOD1 and Hsp70 plus Hsp40. In cells expressing Hsp70 plus Hsp40 or Hsp70 alone, aggregate formation was reduced and neurite outgrowth was improved significantly (arrowheads). The nucleus was stained with propidium iodide (red).

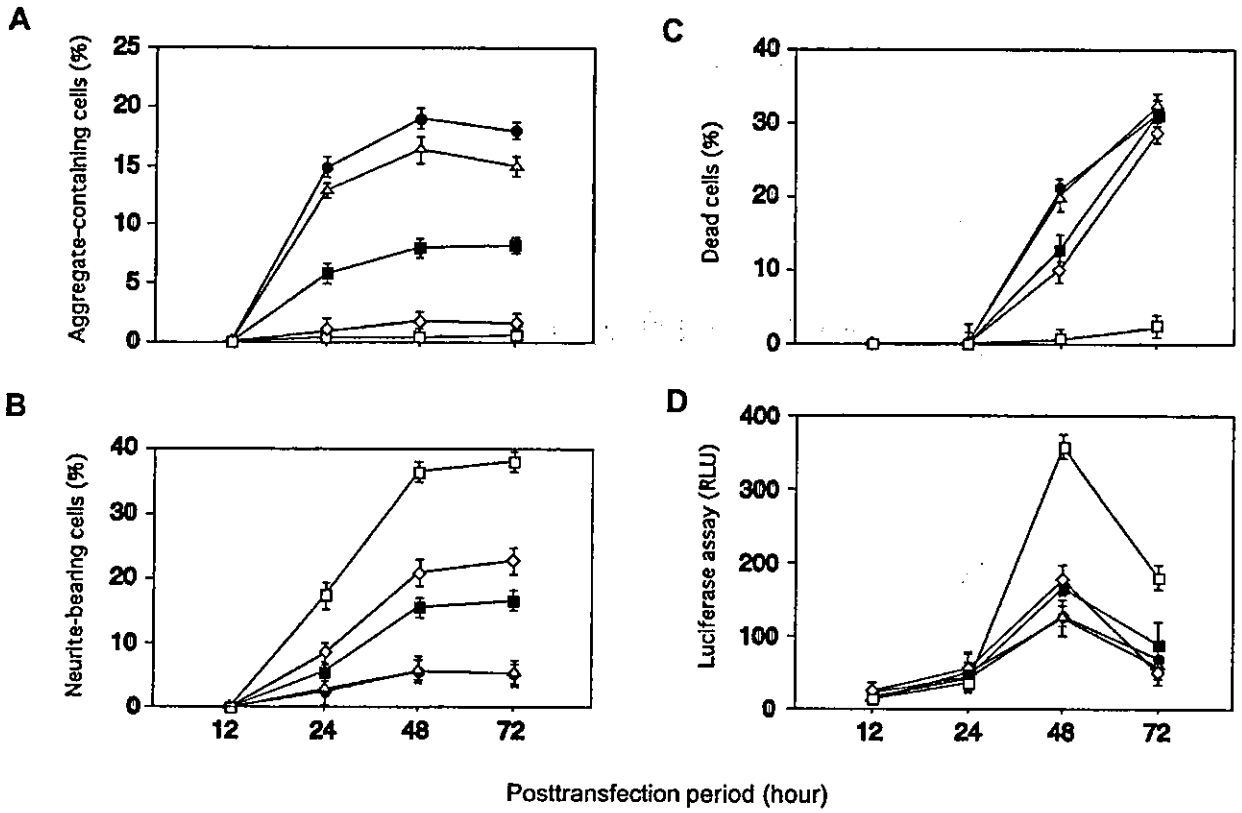

Fig. 3. Frequency of cells with aggregates, frequency of cells bearing neurites, dead cells, and cytotoxic assay. (A) Frequency of intracytoplasmic aggregate-positive cells. Mutant G93A SOD1 induced an intracytoplasmic aggregate formation (wild-type SOD1 versus G93A SOD1, $P<0.0001$ at 24, 48, and 72 h). Hsp70 plus Hsp40 or Hsp70 alone, particularly in the combination of Hsp70 and Hsp40, significantly reduced aggregate formation (Hsp70 or Hsp70+Hsp40 versus G93A SOD1, $P<0.0001$; Hsp70+Hsp40 versus Hsp70, $P<0.005$ at 24, 48, and 72 h). (B) Frequency of cells with neurites exceeding their diameter. The cells expressing mutant SOD1 had few neurites (wild-type SOD1 versus G93A SOD1, $P<0.0001$ at 24, 48, and 72 h). Hsp70 plus Hsp40 or Hsp70 alone, particularly in the combination of Hsp70 and Hsp40, significantly improved neurite outgrowth (Hsp70 or Hsp70+Hsp40 versus G93A SOD1, $P<0.0001$; Hsp70+Hsp40 versus Hsp70, $P<0.005$ at 48 and 72 h). (C) Frequency of dead cells. (D) Luciferase activity of cytotoxic assay. The cell survival rate and luciferase activity were diminished in the cells expressing mutant SOD1 relative to those expressing wild-type SOD1 (wild-type versus G93A SOD1, $P<0.0001$ at 48 and 72 h). Hsp70 plus Hsp40 or Hsp70 alone suppressed cell death and cytotoxicity (Hsp70 or Hsp70+Hsp40 versus G93A SOD1, $P<0.05$ at 48 h).; wild-type SOD1; mutant G93A SOD1; mutant G93A SOD1 and Hsp40; mutant G93A SOD1 and Hsp70; mutant G93A SOD1 and Hsp70 plus Hsp40. Values are the means±S.E.M. for six experiments.

cells expressing mutant SOD1 than in those expressing wild-type SOD1 (Fig. 3B). Almost all the cells containing aggregates showed few neurites (Fig. 7). The cell survival rate and luciferase activity were diminished in the cells expressing mutant SOD1 relative to those expressing wild-type SOD1, and its difference in luciferase activities peaked at 48 h after transfection (Fig. 3C and D). Terminal deoxytransferase-mediated dUTP nick end labeling (TUNEL) assay, however, resulted in negative staining (data not shown).

Western blots demonstrated that SOD1–EGFP protein level was more than 30-fold that of endogenous SOD1 protein level (Fig. 4Aarrow and arrowhead). The protein level of the mutant SOD1–EGFP was consistently less than that of wild-type SOD1–EGFP (Fig. 4A arrowhead). SOD1-immunoreactive, ladder-like, slowly-migrating masses were observed through the gels only in lanes of mutant SOD1 samples (Fig. 4A asterisk). Their molecular weights were approximately two-, three-, and four-fold that of the SOD1–EGFP fusion protein. These protein levels were altered depending on the amount of the applied sample of cell lysate. Since these ladder-like masses were similar to those reported previously [22], we speculated that they were oligomers of the mutant SOD1.

3.2. Endogenous HSPs were upregulated and colocalized with intracytoplasmic aggregates in the cells expressing mutant SOD1

The protein levels of HSPs were examined in transfection experiments. The protein levels of endogenous Hsp70 or Hsp40 were larger in the mutant SOD1-transfected cells than in the non-transfected or the wild-type SOD1-transfected cells (Fig. 5A and B, lanes 1, 2, and 3). These data

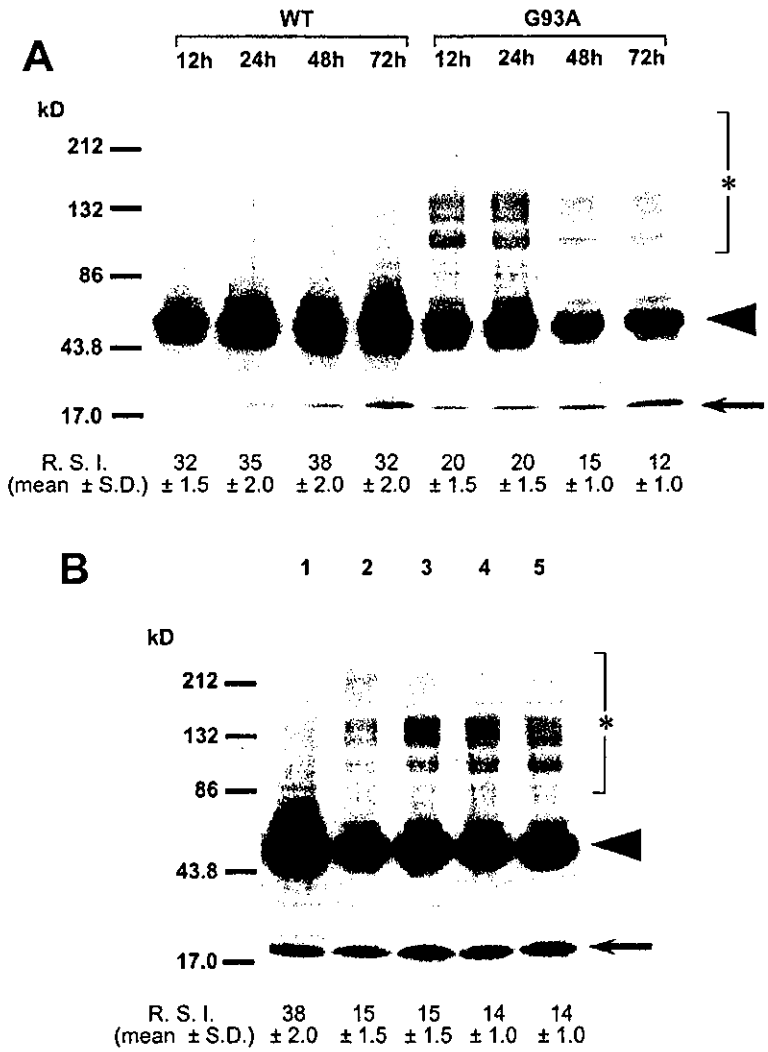

Fig. 4. Protein levels of SOD1–EGFP fusion protein. (A) Protein levels of wild-type and mutant SOD1–EGFP fusion protein. Cells were collected 12, 24, 48, and 72 h after transfection. WT, wild-type SOD1; G93A, mutant G93A SOD1. (B) Protein level of SOD1–EGFP with cotransfected HSPs. Cells were collected 48 h after transfection. Lane 1, Wild-type SOD1 and mock DNA; 2, G93A SOD1 and mock DNA; 3, G93A SOD1 and Hsp70; 4, G93A SOD1 and Hsp40; 5, G93A SOD1 and Hsp70 plus Hsp40. To each well, 20 μg protein of cell lysate was applied. Arrowhead, SOD1–EGFP fusion protein. Arrow, endogenous SOD1. Asterisk, ladder-like, slowly-migrating masses considered as oligomers of mutant SOD1–EGFP fusion protein. Values of RSI are the means±S.E.M. for six experiments.

are in accord with a previous report describing that endogenous Hsp70 was upregulated in cells expressing mutant SOD1 [3]. Cells cotransfected with mutant SOD1 and HSPs showed much larger amounts of Hsp70 or Hsp40 composed of both endogenous and exogenous HSPs (Fig. 5A and B, lanes 4, 5, and 6). Hsp40 was upregulated in the cells cotransfected with mutant SOD1 plus Hsp70 (Fig. 5B, lane 4).

We then assessed whether endogenous HSPs were colocalized with aggregates of mutant SOD1. Laser confocal scanning microscopic analysis demonstrated that the endogenous Hsp70 and Hsp40 were markedly upregulated in the cells containing aggregates and were colocalized with the aggregates of mutant SOD1, while they were hardly detected in the cells expressing wild-type SOD1 (Fig. 6A and B). These data are in accord with a previous report [44].

3.3. Overexpression of Hsp70 and Hsp40 markedly improved neurite outgrowth as it suppressed aggregate formation and cell death

To determine whether overexpression of HSPs is effective in protecting cells against the cellular toxicity of mutant SOD1, we produced cells overexpressing HSPs with mutant SOD1 in the cell model of FALS.

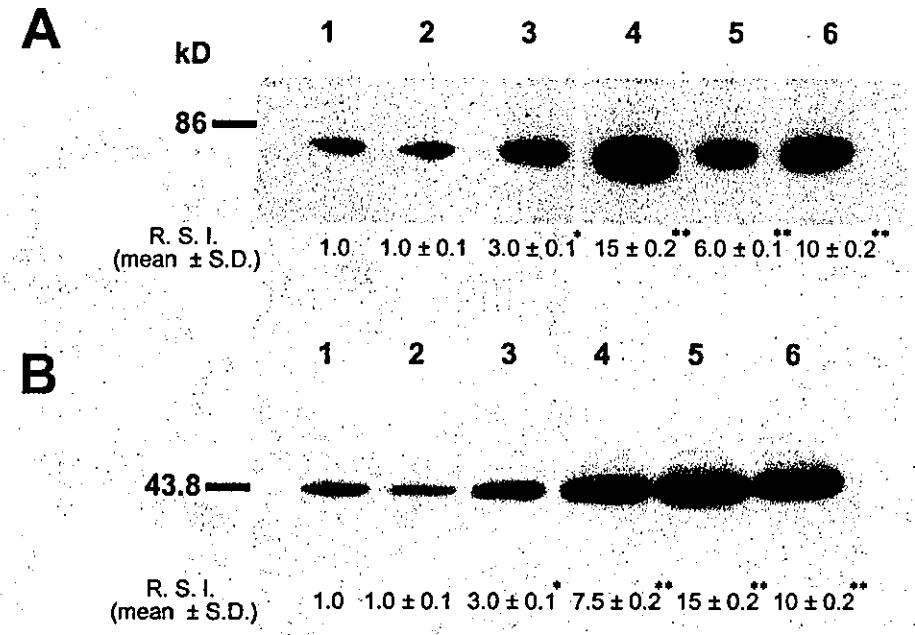

Fig. 5. Protein levels in HSP cotransfection experiments. (A) Protein levels of endogenous and exogenous Hsp70 48 h after transfection. Lane 1, non-transfected; 2, wild-type SOD1 and mock DNA; 3, G93A SOD1 and mock DNA; 4, G93A SOD1 and Hsp70; 5, G93A SOD1 and Hsp40l; 6, G93A SOD1 and Hsp70 plus Hsp40. (B) Protein levels of endogenous and exogenous Hsp40 48 h after transfection. Lane 1, non-transfected; 2, Wild-type SOD1 and mock DNA; 3, G93A SOD1 and mock DNA; 4, G93A SOD1 and Hsp70; 5, G93A SOD1 and Hsp40; 6, G93A SOD1 and Hsp70 plus Hsp40. Cells were collected 48 h after transfection. To each well, 20 μg protein of cell lysate was applied. *$P<0.0001$ versus non-transfected or wild-type SOD1. **$P<0.0001$ versus G93A SOD1. Values of RSI are the means±S.E.M. for six experiments.

Overexpression of Hsp70 plus Hsp40 or Hsp70 alone, particularly in the combination of Hsp70 and Hsp40, significantly reduced aggregate formation (Figs. 2D, 2E and 3A), and markedly improved neurite outgrowth (Figs. 2D, 2E and 3B). Overexpression of Hsp70 plus Hsp40 or Hsp70 alone suppressed cell death (Fig. 3C and D) to a relatively lesser extent than neurite outgrowth or aggregate suppression. Overexpression of Hsp70 plus Hsp40 or Hsp70 alone strikingly changed the aggregates into a diffuse pattern throughout the cytoplasm, and laser confocal scan microscopic analysis demonstrated HSPs colocalized with SOD1–EGFP fusion proteins (Fig. 6A and B). Overexpression of Hsp40 alone was ineffective in suppressing aggregate formation or cell death or in promoting neurite outgrowth (Figs. 2C and 3). In addition, the cells transfected with HSPs or mock DNA only showed neither cellular toxicity nor the proliferating effect (data not shown). Neurite outgrowth was hardly detected in cells containing aggregates (Fig. 7). Moreover, improvement in neurite outgrowth by HSPs was exclusively observed among aggregate-negative cells (Fig. 7). Therefore, the cells with improved neurite outgrowth were considered to be the cells that were prevented aggregate formation by HSPs. Western blots showed that cotransfection with Hsp70 plus Hsp40 or Hsp70 alone did not significantly alter the protein levels of SOD1–EGFP fusion proteins (Fig. 4B arrowhead) or those of the ladder-like, slowly-migrating masses (Fig. 4B asterisk).

4. Discussion

This is the first demonstration that overexpression of HSPs, especially the combination of Hsp70 and Hsp40, improved neurite outgrowth as it suppressed both intracytoplasmic aggregate formation and cell death in a cultured neuronal cell model of FALS.

The abnormal morphology and inhibition of neurite outgrowth in mutant SOD1-transfected cells are intriguing because the degeneration of neuronal processes in motor neurons also occurs in FALS [18,19]. This inhibition of neurite outgrowth might correspond to the axonal degeneration (including impaired axonal transport) detected in mutant SOD1 transgenic mice [1,9,49,51]. The lack of normal neurite outgrowth might reflect the dysfunction of molecules or proteins that are important for maintaining a normal neuronal process [27]. Overexpression of HSPs strikingly changed the aggregates into a diffuse pattern throughout the cytoplasm and improved neurite outgrowth. Our study also demonstrated that neurite outgrowth was hardly detected in cells containing intracytoplasmic aggregates, whereas it was detected almost exclusively in cells without aggregate formation. Thus, aggregate formation was suggested to play a causative role in cellular dysfunction such as the inhibition of neurite outgrowth. Western blots indicated that the endogenous HSPs were self-defensively upregulated in cells expressing mutant SOD1 as previously reported [3], but they did not seem to be

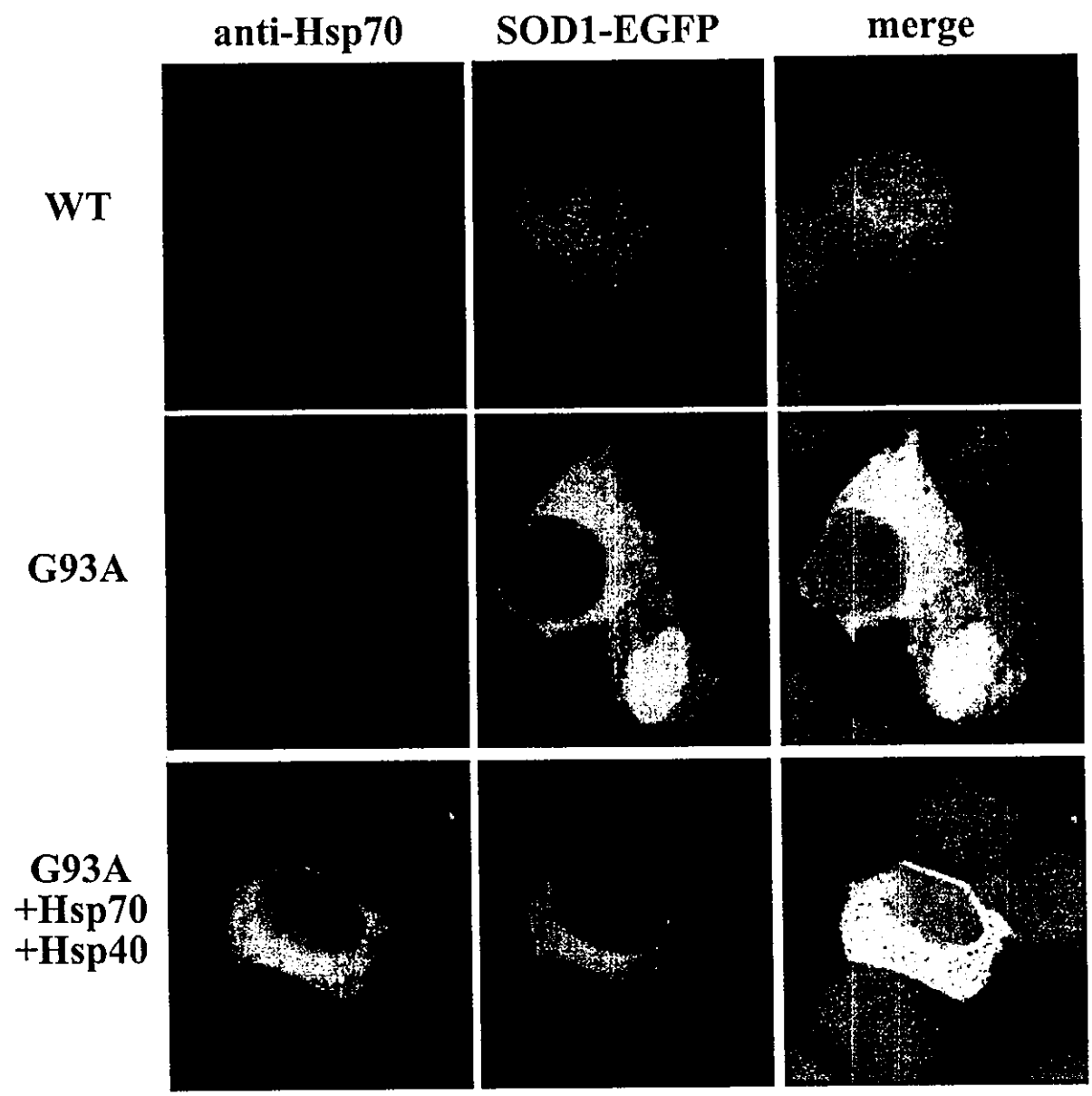

Fig. 6. Endogenous HSPs colocalized with intracytoplasmic aggregates and transfected HSPs dispersed throughout the cytoplasm with SOD1–EGFP fusion protein. Overlays of the three images were taken by laser confocal microscopy 48 h after transfection. (A) Immunofluorescent stain of Hsp70. (B) Immunofluorescent stain of Hsp40. Each endogenous Hsp70 (red in A) and endogenous Hsp40 (red in B) was upregulated and colocalized with aggregates (green) in cells with mutant G93A SOD1. Cells cotransfected with Hsp70 and Hsp40 showed diffuse positive staining throughout the cytoplasm (red). The nucleus was stained with TOTO-3 (blue). WT, wild-type SOD1; G93A, mutant G93A SOD1; G93A+Hsp70+Hsp40, mutant G93A SOD1 cotransfected with Hsp70 plus Hsp40.

numerous enough to protect cells against the toxicity of mutant SOD1 without overexpression of exogenous HSPs. Microscopic analysis showed that HSPs obviously diminished aggregate formation, but that the ladder-like masses on the Western blots, which we considered as oligomers of mutant SOD1–EGFP fusion proteins, did not significantly change even in the cells overexpressing HSPs. A previous study indicated that coexpression of Hsp70 by microinjection promoted the viability of motor neurons expressing G93A SOD1 to some extent in the early phase, although the toxic effects of the mutant SOD1 were obvious at a later time despite strong suppressing of aggregate formation [3]. The limited effect of HSPs on cell survival in our model was in accord with this previous report [3], and it may be correlated with the ladder-like masses detected by Western blots. Another report suggested that the increase in mutant SOD1 oligomers might disrupt microtubule-dependent axonal transport [22]. As to

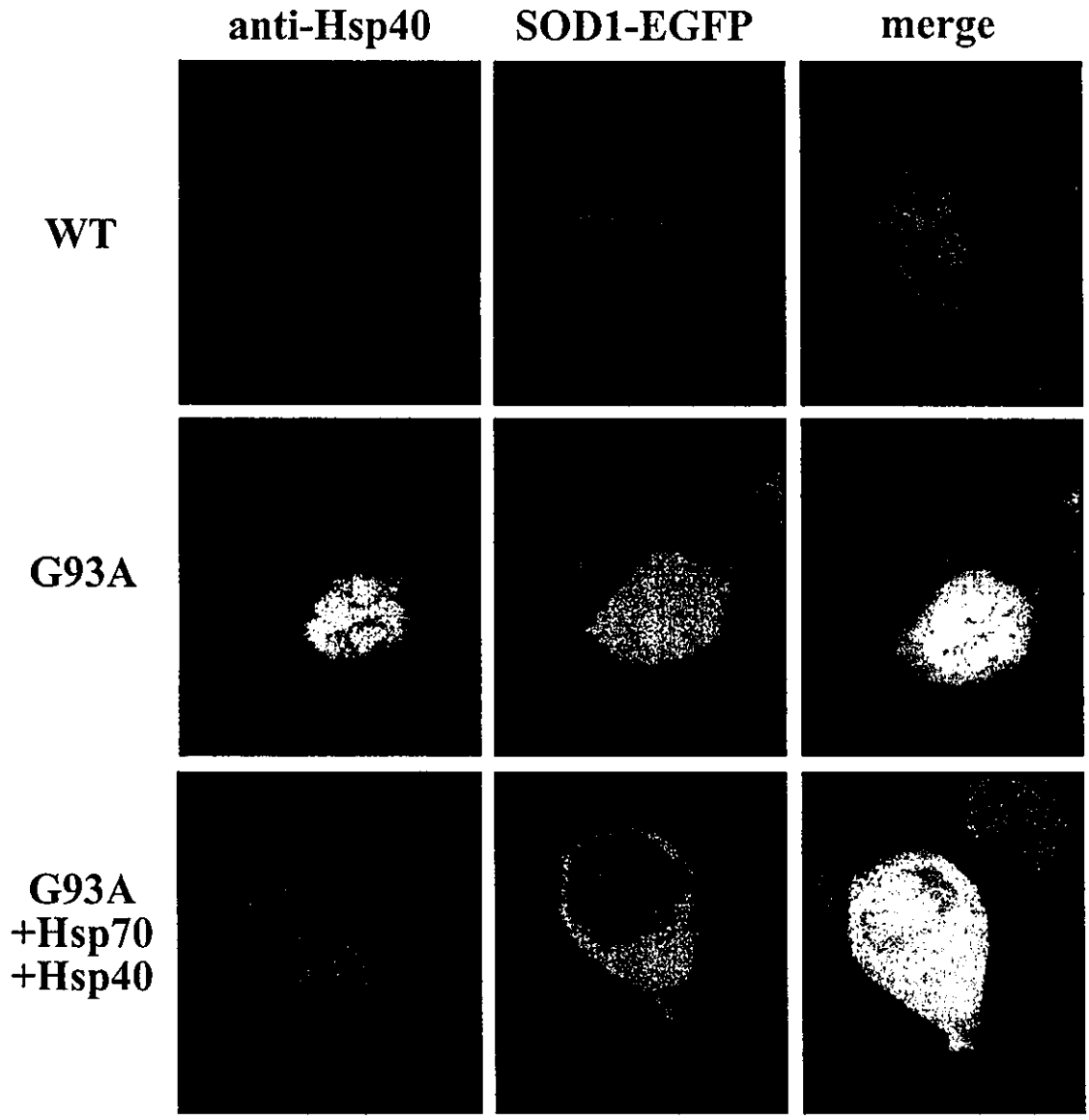

Fig. 6. (*continued*)

its crystal structure, SOD1 has a β-barrel structure that consists of eight antiparallel β-sheets [34]. Mutation in a β-sheet protein was considered to accelerate its oligomeric formation [45], and the toxicity of oligomers of mutant proteins with β-sheets for cell survival has been observed in amyloid-protein of Alzheimer's disease [26,35]. The correlation between neuronal death and oligomeric formation of mutant SOD1 still remains to be investigated.

The major question is the relationship among the large aggregates, cell survival and neurite outgrowth. It has been controversial whether the large aggregates are toxic [4] or provide self-defense [16,21,22,25] for the cells with mutant SOD1. Our observation suggests that large aggregates, suppressed by the overexpression of HSPs, may be more correlated with cell dysfunction such as neurite outgrowth rather than cell death. Mutant proteins accumulating during the normal cellular disposal processes may result in cellular dysfunctions when the accumulation exceeds the cellular capacity [40]. On the other hand, expression of the mutant SOD itself may alter the cellular function including transcriptional activity independent of aggregate formation, as has been proposed in the polyglutamine diseases [28,29,43]. A wide range of neuronal dysfunctions and cell death have so far been observed in the in vitro and in vivo models of FALS with mutant SOD1, including defective axonal transport [1,9,49,51], neurofilament accumulation [41,42,51], fragmentation of the Golgi apparatus [15,32,47,51], mitochondrial dysfunction [6,24], and in-

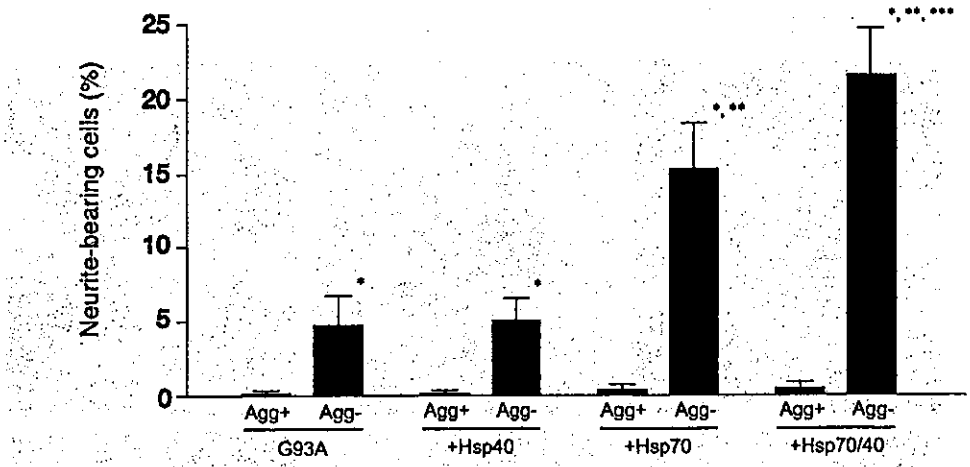

Fig. 7. Frequency of neurite outgrowth in the aggregate-containing cells or the aggregate-negative cells. G93A, mutant G93A SOD1; +Hsp40, mutant G93A SOD1 cotransfected with Hsp40; +Hsp70, mutant G93A SOD1 cotransfected with Hsp70; +Hsp70/40, mutant G93A SOD1 cotransfected with Hsp70 plus Hsp40; Agg+, aggregate-containing cell; Agg−, aggregate-negative (but EGFP-positive) cell. Assessment was carried out 48 h after transfection. *$P<0.0001$, aggregate-containing cell versus aggregate-negative cells among each group; **$P<0.0001$, G93A versus+Hsp70 or +Hsp70/40; ***$P<0.005$, +Hsp70 versus+Hsp70/40. Values are the means±S.E.M. for six experiments.

creased susceptibility to cell death due to various stresses such as the free radicals, oxidative stress and excitotoxin [2,13,37,38,50]. Although some of these cellular events, particularly those of cellular dysfunction, could be related to the aggregate formation that can be prevented by the overexpression of HSPs, the major part of the molecular basis of mutant SOD1 toxicity still remains to be elucidated. Finally, we demonstrated that HSPs may play an important role in intracytoplasmic aggregate formation in FALS, ameliorate cell dysfunction, and be useful in the treatment for FALS.

Acknowledgements

This work was supported by grants from the Ministry of Health, Labor and Welfare of Japan, and a Center of Excellence Grant from the Ministry of Education, Culture, Sports, Science and Technology of Japan.

References

[1] D.R. Borchelt, P.C. Wong, M.W. Becher, C.A. Pardo, M.K. Lee, Z.S. Xu, G. Thinakaran, N.A. Jenkins, N.G. Copeland, S.S. Sisodia, D.W. Cleveland, D.L. Price, P.N. Hoffman, Axonal transport of mutant superoxide dismutase 1 and focal axonal abnormalities in the proximal axons of transgenic mice, Neurobiol. Dis. 5 (1998) 27–35.

[2] L.A. Bristol, J.R. Rothstein, Glutamine transporter gene expression in amyotrophic lateral sclerosis motor cortex, Ann. Neurol. 39 (1996) 676–679.

[3] W. Bruening, J. Roy, B. Giasson, D.A. Figlewicz, W.E. Mushynski, H.D. Durham, Up-regulation of protein chaperones preserves viability of cells expressing toxic Cu/Zn-superoxide dismutase mutants associated with amyotrophic lateral sclerosis, J. Neurochem. 72 (1999) 693–699.

[4] L.I. Bruijin, M.K. Houseweart, S. Kato, K.L. Anderson, S.D. Anderson, E. Ohama, A.G. Reaume, R.W. Scott, D.W. Cleveland, Aggregation and motor neuron toxicity of an ALS-linked SOD1 mutant independent from wild-type SOD1, Science 281 (1998) 1851–1854.

[5] K.T. Bukau, A.L. Horwich, The Hsp70 and Hsp60 chaperone machines, Cell 92 (1998) 351–366.

[6] M.T. Carrì, A. Ferri, A. Battistoni, L. Famhy, R. Gabbianelli, F. Poccia, G. Rotilio, Expression of a Cu,Zn superoxide dismutase typical of familial amyotrophic lateral sclerosis induces mitochondrial alteration and increase of cytosolic Ca^{2+} concentration in transfected neuroblastoma SH-SY5Y cells, FEBS Lett. 414 (1997) 365–368.

[7] Y. Chai, S.L. Koppenhafer, N.M. Bonini, H.L. Paulson, Analysis of the role of heat shock protein (Hsp) molecular chaperones in polyglutamine disease, J. Neurosci. 19 (1999) 10338–10347.

[8] H.Y.E. Chan, J.M. Warrick, G.L. Gray-Board, H.L. Paulson, N.M. Bonini, Mechanism of chaperone suppression of polyglutamine disease: selectivity, synergy and modulation of protein solubility in *Drosophila*, Hum. Mol. Genet. 9 (2000) 2811–2820.

[9] J.F. Collard, F. Côte, J.P. Julien, Defective axonal transport in a transgenic mouse model of amyotrophic lateral sclerosis, Nature 375 (1995) 61–64.

[10] C.J. Cummings, M.A. Mancini, B. Antalffy, D.B. DeFranco, H.T. Orr, H.Y. Zoghbi, Chaperone suppression of aggregation and altered subcellular proteasome localization imply protein misfolding in SCA1, Nature Genet. 19 (1998) 148–154.

[11] J.R. de Wet, K.V. Wood, M. DeLuca, D.R. Helinski, S. Subramani, Firefly luciferase gene structure and expression in mammalian cells, Mol. Cell. Biol. 7 (1987) 725–737.

[12] H.D. Durham, J. Roy, L. Dong, D.A. Figlewicz, Aggregation of mutant Cu/Zn superoxide dismutase proteins in culture model of ALS, J. Neuropathol. Exp. Neurol. 56 (1997) 523–530.

[13] A. Ferri, R. Gabbianelli, A. Casciati, E. Paolucci, G. Rotilio, M.T. Carrì, Calcineurin activity is regulated both by redox compounds and by mutant familial amyotrophic lateral sclerosis–superoxide dismutase, J. Neurochem. 75 (2000) 606–613.

[14] J. Frydman, E. Nimmesgern, K. Ohtsuka, F.U. Hartl, Folding of nascent polypeptide chains in a high molecular mass assembly with molecular chaperones, Nature 370 (1994) 111–117.

[15] Y. Fujita, K. Okamoto, A. Sakurai, N.K. Gonatas, A. Hirano,

Fragmentation of the Golgi apparatus of the anterior horn cells in patients with familial amyotrophic lateral sclerosis with SOD1 mutations and posterior column involvement, J. Neurol. Sci. 147 (2000) 137–140.

[16] R. García-Mata, Z. Bebök, E.J. Sorscher, E.S. Sztul, Characterization and dynamics of aggresome formation by a cystolic GFP-chimera, J. Cell Biol. 146 (1999) 1239–1254.

[17] F.U. Hartl, Molecular chaperone in cellular protein folding, Nature. 381 (1996) 571–580.

[18] A. Hirano, L.T. Kurland, G.P. Sayre, Familial amyotrophic lateral sclerosis, Arch. Neurol. 16 (1967) 232–243.

[19] A. Hirano, Neuropathology of ALS: an overview, Neurology 47 (Suppl. 2) (1996) S63–S66.

[20] H. Ikeda, M. Yamaguchi, S. Sugai, Y. Aze, S. Narumiya, A. Kakizuka, Expanded polyglutamine in the Machado–Joseph disease protein induces cell death in vitro and in vivo, Nature Genet. 13 (1996) 196–202.

[21] J.A. Johnston, C.L. Ward, R.R. Kopito, Aggresome: a cellular response to misfolded proteins, J. Cell Biol. 143 (1998) 1883–1898.

[22] J.A. Johnston, M.J. Dalton, M.E. Gurney, R.R. Kopito, Formation of high molecular weight complexes of mutant Cu,Zn-superoxide dismutase in a mouse model for familial amyotrophic lateral sclerosis, Proc. Natl. Acad. Sci. USA 97 (2000) 12571–12576.

[23] Y. Kobayashi, A. Kume, M. Li, M. Doyu, M. Hata, K. Ohtsuka, G. Sobue, Chaperones Hsp70 and Hsp40 suppress aggregate formation and apoptosis in cultured neuronal cells expressing truncated androgen receptor protein with expanded polyglutamine tract, J. Biol. Chem. 275 (2000) 8772–8778.

[24] J. Kong, Z. Xu, Massive mitochondrial degeneration in motor neurons triggers the onset of amyotrophic lateral sclerosis in mice expressing a mutant SOD1, J. Neurosci. 18 (1998) 3241–3250.

[25] R.R. Kopito, Aggresome, inclusion bodies and protein aggregation, Trends Cell Biol. 10 (2000) 524–530.

[26] M.P. Lambert, A.K. Barlow, B.A. Chromy, C. Edwards, R. Freed, M. Liosatos, T.E. Morgan, I. Rozovsky, B. Trommer, K.L. Viola, P. Wals, C. Zhang, C.E. Finch, G.A. Krafft, W.L. Klein, Diffusible, nonfibrillar ligands derived from Aβ1–42 are potent central nervous system neurotoxins, Proc. Natl. Acad. Sci. USA 95 (1998) 6448–6453.

[27] S.H. Li, A.L. Cheng, H. Li, X.J. Li, Cellular defects and altered gene expression in PC12 cells stably expressing mutant huntingtin, J. Neurosci. 19 (1999) 5159–5172.

[28] X. Lin, B. Antalffy, D. Kang, H.T. Orr, H.Y. Zoghbi, Polyglutamine expansion downregulates specific neuronal genes before pathologic changes in SCA1, Nat. Neurosci. 3 (2000) 157–163.

[29] A. McCampbell, J.P. Taylor, A.A. Taye, J. Robitschek, M. Li, J. Walcott, D. Merry, Y. Chai, H. Paulson, G. Sobue, K.H. Fischbeck, CREB-binding protein sequestration by expanded polyglutamine, Hum. Mol. Genet. 9 (2000) 2197–2202.

[30] A.A. Michels, B. Kanon, A.W.T. Konings, K. Ohtsuka, O. Bensaude, H.H. Kampinga, Hsp70 and Hsp40 chaperone activities in the cytoplasm and the nucleus of mammalian cells, J. Biol. Chem. 272 (1997) 33283–33289.

[31] Y. Minami, J. Höhfeld, K. Ohtsuka, F. Hartl, Regulation of heat-shock protein 70 reaction cycle by the mammalian DnaJ homolog, Hsp40, J. Biol. Chem. 271 (1996) 19617–19624.

[32] Z. Mourelatos, N.K. Gonatas, A. Stieber, M.E. Gurney, M.C. Dal Canto, The Golgi apparatus of spinal cord motor neurons in transgenic mice expressing mutant Cu,Zn superoxide dismutase becomes fragmentated in early, preclinical stages of the disease, Proc. Natl. Acad. Sci. USA 93 (1996) 5472–5477.

[33] K. Ohtsuka, T. Suzuki, Roles of molecular chaperones in the nervous system, Brain Res. Bull. 53 (2000) 141–146.

[34] J. Richardson, K.A. Thomas, B.H. Rubin, D.C. Richardson, Crystal structure of bovine Cu,Zn superoxide dismutase at 3 A resolution: chain tracing and metal ligands, Proc. Natl. Acad. Sci. USA 72 (1975) 1349–1353.

[35] A.E. Roher, M.O. Chaney, Y.-M. Kuo, S.D. Webster, W.B. Stine, L.J. Haverkamp, A.S. Woods, R.J. Cotter, J.M. Tuohy, G.A. Krafft, B.S. Bonnell, M.R. Emmerling, Morphology and toxicity of A-(1–42) dimer derived from neuritic and vascular amyloid deposits of Alzheimer's disease, J. Biol. Chem. 271 (1996) 20631–20635.

[36] D.R. Rosen, T. Siddique, D. Patterson, D.A. Figlewicz, P. Sapp, A. Hentati, D. Donaldson, J. Goto, J.P. O'Regan, H.X. Deng, Z. Rahmani, A. Krizus, D. McKenna-Yasek, A. Cayabyab, S.M. Gaston, R. Berger, R.E. Tanzi, J.J. Halperin, B. Herzfeldt, R.V. den Bergh, W.Y. Hung, T. Bird, G. Deng, D.W. Mulder, C. Smyth, N.G. Laing, E. Soriano, M.A. Pericak-Vance, J. Haines, G.A. Rouleau, J.S. Gusella, H.R. Horvitz, R.H. Brown, Mutations in Cu/Zn superoxide dismutase gene are associated with familial amyotrophic lateral sclerosis, Nature 362 (1993) 59–62.

[37] J.D. Rothstein, M. Van Kammen, A.I. Levey, L.J. Martin, R.W. Kuncl, Selective loss of glial glutamine transporter GLT-1 in amyotrophic lateral sclerosis, Ann. Neurol. 38 (1995) 73–84.

[38] J.D. Rothstein, M. Dykes-Hoberg, C.A. Pardo, L.A. Bristol, L. Jin, R.W. Kuncl, Y. Kanai, M.A. Hediger, Y. Wang, J.P. Schielke, D.F. Welty, Knockout of glutamine transporters reveals a major role for astroglial transport in excitotoxicity and clearance of glutamine, Neuron 16 (1996) 675–686.

[39] A.L. Schwartz, A. Ciechanover, The ubiquitin–proteasome pathway and pathogenesis of human disease, Annu. Rev. Med. 50 (1999) 57–74.

[40] M.Y. Sherman, A.L. Goldberg, Cellular defenses against unfolded proteins; a cell biologist thinks about neurodegenerative diseases, Neuron 29 (2001) 15–32.

[41] N. Shibata, A. Hirano, M. Kobayashi, T. Siddique, H.X. Deng, W.Y. Hung, T. Kato, K. Asayama, Intense superoxide dismutase-1 immunoreactivity in intracytoplasmic hyaline inclusion of familial amyotrophic lateral sclerosis with posterior column involvement, J. Neuropathol. Exp. Neurol. 55 (1996) 481–490.

[42] N. Shibata, A. Hirano, M. Kobayashi, M.C. Dal Canto, M.E. Gurney, T. Komori, T. Umahara, K. Asayama, Presence of Cu/Zn superoxide dismutase (SOD) immunoreactivity in neuronal hyaline inclusions in spinal cords from mice carrying a transgene for Gly93Ala mutant human Cu/Zn SOD, Acta Neuropathol. 95 (1998) 136–142.

[43] T. Shimohata, T. Nakajima, M. Yamada, C. Uchida, O. Onodera, S. Naruse, T. Kimura, R. Koide, K. Nozaki, Y. Sano, H. Ishiguro, K. Sakoe, T. Ooshima, A. Sato, T. Ikeuchi, M. Oyake, T. Sato, Y. Aoyagi, I. Hozumi, T. Nagatsu, Y. Takiyama, M. Nishizawa, J. Goto, I. Kanazawa, I. Davidson, N. Tanese, H. Takahashi, S. Tsuji, Expanded polyglutamine stretches interact with TAFII 130, interfering with CREB-dependent transcription, Nature Genet. 26 (2000) 29–36.

[44] G.A. Shinder, M.C. Lacourse, S. Minotti, H.D. Durham, Mutant Cu/Zn-superoxide dismutase proteins have altered solubility and interact with heat shock/stress proteins in models of amyotrophic lateral sclerosis, J. Biol. Chem. 276 (2001) 12791–12796.

[45] M.A. Speed, D.I.C. Wang, J. King, Specific aggregation of partially folded polypeptide chains: the molecular basis of inclusion body composition, Nat. Biotechnol. 14 (1996) 1283–1287.

[46] D. Stenoien, C. Cummings, H. Adams, M. Mancini, K. Patel, G. DeMartino, M. Marcelli, N. Weigel, M. Mancini, Polyglutamine-expanded androgen receptors form aggregates that sequester heat shock proteins, proteasome components and SRC-1, and are suppressed by the HDJ-2 chaperone, Hum. Mol. Genet. 8 (1999) 731–741.

[47] A. Stieber, J.O. Gonatas, N.K. Gonatas, Aggregation of ubiquitin and a mutant ALS-linked SOD1 protein correlate with disease progression and fragmentation of the Golgi apparatus, J. Neurol. Sci. 173 (2000) 53–62.

[48] K. Umesono, K.K. Murakami, C.C. Thompson, R.M. Evans, Direct repeats as selective response elements for the thyroid hormone, retinoic acid, and vitamin D3 receptors, Cell 65 (1991) 1255–1266.

[49] H. Warita, Y. Itoyama, K. Abe, Selective impairment of fast anterograde axonal transport in the peripheral nerves of asymptomatic transgenic mice with a G93A mutant SOD1 gene, Brain Res. 819 (1999) 120–131.

[50] M.B. Yim, J.H. Kang, H.S. Yim, H.S. Kwak, P.B. Chock, E.R. Stadtman, A gain-of-function of an amyotrophic lateral sclerosis-associated Cu,Zn-superoxide dismutase mutant: an enhancement of free radical formation due to a decrease in Km for hydrogen peroxide, Proc. Natl. Acad. Sci. USA 93 (1996) 5709–5714.

[51] B. Zhang, P.H. Tu, F. Abtahian, J.Q. Trojanowski, V.M.Y. Lee, Neurofilaments and orthograde transport are reduced in ventral root axons of transgenic mice that express human SOD1 with a G93A mutation, J. Cell Biol. 139 (1997) 1307–1315.

Neuron, Vol. 35, 843–854, August 29, 2002, Copyright ©2002 by Cell Press

Testosterone Reduction Prevents Phenotypic Expression in a Transgenic Mouse Model of Spinal and Bulbar Muscular Atrophy

Masahisa Katsuno,[1,4] Hiroaki Adachi,[1,4]
Akito Kume,[1] Mei Li,[1] Yuji Nakagomi,[2]
Hisayoshi Niwa,[1] Chen Sang,[1] Yasushi Kobayashi,[1]
Manabu Doyu,[1] and Gen Sobue[1,3]
[1]Department of Neurology
Nagoya University Graduate School of Medicine
65 Tsurumai-cho
Showa-ku, Nagoya 466-8550
Japan
[2]Laboratory of Electron Microscopy
Aichi Medical University
21 Karimata, Yazako
Nagakute-cho, Aichi 480-1195
Japan

Summary

Spinal and bulbar muscular atrophy (SBMA) is a polyglutamine disease caused by the expansion of a CAG repeat in the *androgen receptor* (*AR*) gene. We generated a transgenic mouse model carrying a full-length *AR* containing 97 CAGs. Three of the five lines showed progressive muscular atrophy and weakness as well as diffuse nuclear staining and nuclear inclusions consisting of the mutant AR. These phenotypes were markedly pronounced in male transgenic mice, and dramatically rescued by castration. Female transgenic mice showed only a few manifestations that markedly deteriorated with testosterone administration. Nuclear translocation of the mutant AR by testosterone contributed to the phenotypic difference with gender and the effects of hormonal interventions. These results suggest the therapeutic potential of hormonal intervention for SBMA.

Introduction

Spinal and bulbar muscular atrophy (SBMA) is an X-linked late-onset motor neuron disease characterized by proximal muscle atrophy, weakness, contraction fasciculations, and bulbar involvement (Kennedy et al., 1968; Sobue et al., 1989). Heterozygous female carriers are usually asymptomatic, although some express subclinical phenotypes, including high amplitude motor unit potentials on electromyography (Sobue et al., 1993; Mariotti et al., 2000). A specific treatment for SBMA has not been established. Testosterone may improve motor function in some patients, although it has no effects on the progression of SBMA (Danek et al., 1994; Goldenberg and Bradley, 1996; Neuschmid-Kaspar et al., 1996).

The molecular basis of SBMA is the expansion of a trinucleotide CAG repeat in the first exon of the *androgen receptor* (*AR*) gene, which encodes the polyglutamine (polyQ) tract (La Spada et al., 1991). Thus, SBMA was the first described member of polyQ diseases including Huntington's disease (HD), several forms of spinocerebellar ataxia, and dentatorubral and pallidoluysian atrophy (DRPLA) (Zoghbi and Orr, 2000; Paulson, 2000). These polyQ diseases share several clinical findings such as anticipation, somatic mosaicism (Tanaka et al., 1999), and selective neuronal and non-neuronal involvement despite widespread expression of the mutant gene (Zoghbi and Orr, 2000; Paulson, 2000). There is also an inverse correlation between the CAG repeat size and the age at onset, or the disease severity adjusted by the age at examination in SBMA (Doyu et al., 1992; La Spada et al., 1992; Igarashi et al., 1992) as well as other polyQ diseases (Duyao et al., 1993; Orr et al., 1993; Zoghbi and Orr, 2000; Paulson, 2000).

Previously, we reported nuclear inclusions (NIs) containing the mutant and truncated AR with expanded polyQ in the residual motor neurons in the brain stem and spinal cord (Li et al., 1998a) as well as in the skin, testis, and some other visceral organs of SBMA patients (Li et al., 1998b). The presence of NIs is a pathologic hallmark of most other polyQ diseases, and is considered to be relevant to pathophysiology (Zoghbi and Orr, 2000; Paulson, 2000). However, considerable controversy surrounds the importance of NIs in the pathophysiology of the polyQ diseases (Klement et al., 1998; Saudou et al., 1998; Cummings et al., 1999; Gutekunst et al., 1999). NIs may reflect a cellular mechanism that protects neurons from the toxic effects of polyQ tract, and nuclear translocation of the mutant protein may be essential in the pathophysiology of the majority of polyQ diseases. SBMA is unique among these disorders in that the mutant protein, AR, has a specific ligand, testosterone, and this ligand alters the subcellular localization of the protein by favoring its nuclear uptake. The AR is normally confined to a multi-heteromeric inactive complex in the cell cytoplasm, and translocates into the nucleus in a ligand-dependent manner (Zhou et al., 1994), which is likely enhanced in male SBMA patients. We took advantage of this ligand effect to study the role of nuclear uptake of the mutant protein on the disease manifestations in transgenic (Tg) mice.

Unlike the profound gender difference of phenotypes in SBMA patients, neither a Tg mouse model of SBMA expressing expanded pure 239 CAGs under the control of human AR promoter (Adachi et al., 2001) nor that carrying truncated *AR* with 112 CAGs (Abel et al., 2001) showed any remarkable phenotypic difference with gender. In the present study, we generated Tg mice with full-length *AR* containing 97 CAGs, showing neurologic phenotypes with significant sexual differences. Our findings reiterate the importance of nuclear localization of the mutant protein in the disease mechanism, and indicate an approach to effective treatment for SBMA.

Results

Tg Mice Carrying Full-Length Human *AR* with 97 CAGs Showed Sexual Differences in Symptoms, Transgene Expression, and Pathology

Symptomatic difference with gender: we generated Tg mice expressing the full-length human *AR* containing

[3]Correspondence: sobueg@med.nagoya-u.ac.jp
[4]These authors contributed equally to this work.

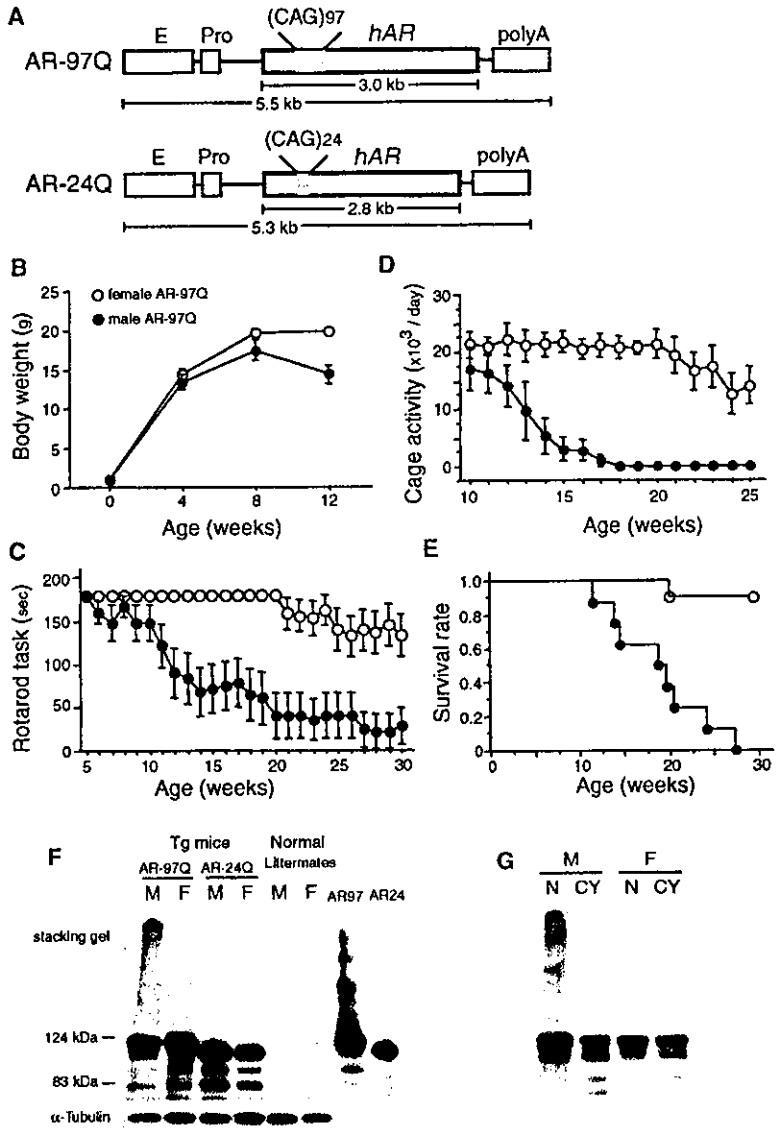

Figure 1. Sexual Differences in Symptomatic Phenotypes and Transgene Expression

(A) Schematic view of the transgene constructs. The microinjected fragment was composed of a cytomegalovirus enhancer (E), a chicken β-actin promoter (Pro), a full-length human *AR* containing 24 or 97 CAGs (*hAR*), and a rabbit β-globin polyadenylation signal sequence (polyA). (B, C, D, and E) Sexual differences in body weight (B, #2–6), rotarod task (C, #7–8), cage activity (D, #2–6), and survival rate (E, #7–8). All parameters are significantly different between the male AR-97Q mice (●, n = 8) and female AR-97Q mice (○, n = 8) ($p = 0.001$, $p = 0.003$, $p = 0.005$, and $p = 0.001$, respectively). (F) Western blot analysis of total homogenates from the muscle of the male (M) and female (F) mice of AR-97Q, AR-24Q, and normal littermates (12-week-old) immunolabeled by an antibody (N-20) against AR. Mouse AR was hardly detectable in the normal littermates. Comparison with muscle extracts from normal littermates indicated that most of the lower bands in transgenic (Tg) mice represent truncated human AR. Protein lysate from Neuro2a cells transfected with the transgene containing 24 CAGs and that with 97 CAGs (AR24 and AR97) are shown for size comparison. (G) Western blot analysis of nuclear (N) and cytoplasmic (CY) fractions from the muscle of the male (M) and female (F) AR-97Q mice (#7–8, 14-week-old) immunolabeled by N-20.

24 or 97 CAGs under the control of a cytomegalovirus enhancer and a chicken β-actin promoter (Figure 1A). We established 3 lines with 24 glutamines (AR-24Q) and 5 lines with 97 glutamines (AR-97Q). Copy numbers of the transgene were 1 to 5 in AR-24Q mice and 1 to 3 in AR-97Q mice (Table 1). We assessed the 24 or 97 CAG repeat in the transgene by the PCR amplification on the tail DNA using a fluorescently labeled primer, and subsequent size determination on the polyacrylamide gel did not show unequivocal intergenerational instability in the CAG repeat number (data not shown).

Three of five lines with AR-97Q (#2–6, #4–6, #7–8) exhibited progressive motor impairment, although no lines with AR-24Q showed any manifested phenotypes up to the latest age examined, 30 weeks old. All three symptomatic lines showed small body size, short life span, progressive muscle atrophy and weakness, as well as reduced cage activity, all of which were markedly pronounced and accelerated in the male AR-97Q mice, but not observed or far less severe in the female AR-97Q mice regardless of the line (Figures 1B–1E). The first detectable phenotype is muscle atrophy of the trunk and hindlimbs followed by weight loss and impairment of the rotarod task. We detected the onset of motor impairment by the rotarod task at 8 to 9 weeks of age in the male AR-97Q mice, while 15 weeks or more in the females (Table 1). The affected mice were hypoactive and dragged their hindlimbs. The forelimbs were not involved until hindlimb atrophy became severe. Males showed a markedly faster and earlier motor deficit than females, and shorter life span. The 50% mortality ranged from 66 to 132 days of age in the male AR-97Q mice of 3 lines, whereas mortality of the female AR-97Q mice remained only 10% to 30% at more than 210 days in the 3 lines. The cause of death was cachexia due to hyponutrition and dehydration.

Expression of transgene: Western blot analysis revealed the transgenic protein retained in the stacking gel as well as a single band of AR monomer consistent with 97 glutamines and truncated fragments of mutant

Table 1. Phenotypes of Transgenic Mice

Line	Copy Number	Onset of Weight Loss (Weeks)	Onset of Rotarod Impairment (Weeks)	Median Life Expectancy (Days)	1C2 Staining
AR-97Q					
2–6	1–3	6/16	9/18	66/>210	++/+
4–6	1–3	4/12	8/15	110/>210	++/+
7–8	1–3	8/16	9/21	132/>210	++/+
3–7	ND	8/–	–/–	>210	ND
8–5	ND	8/–	–/–	>210	ND
AR-24Q					
5–5	5	–/–	–/–	ND	–/–
8–7	1–3	–/–	–/–	ND	
12–13	1–3	–/–	–/–	ND	ND

Data is shown as male/female. –, not detected; +, detectable diffuse nuclear staining and nuclear inclusions; ++, abundant diffuse nuclear staining and nuclear inclusions; ND, not determined. All mice were examined until 30 weeks old.

AR in all symptomatic lines. We detected these proteins in the spinal cord, cerebrum, heart, muscle, and pancreas. Although the male AR-97Q mice had more protein within the stacking gel than the female AR-97Q mice, the female AR-97Q mice had more monomeric AR protein (Figure 1F). AR-24Q mice showed a single band of AR with 24 glutamines without protein in the stacking gel. The nuclear fraction contained the most transgene protein within the stacking gel (Figure 1G).

There was no significant difference in the expression of the mRNA of the transgene between the male and female AR-97Q mice (data not shown). These observations indicate that the nuclear localization is the major expression profile of the transgene protein in the stacking gel. This nuclear localization was more prominent in males than in females, while the mRNA expression levels were indistinguishable between genders.

Pathology: AR-24Q mice showed no pathologic abnormalities at the age of 12 weeks. In AR-97Q mice, we detected diffuse nuclear staining and less frequent NIs with 1C2, an antibody specifically recognizing the expanded polyQ (Trottier et al., 1995), in the neurons of the spinal cord, cerebrum, cerebellum, brain stem, and dorsal root ganglia as well as non-neuronal tissue such as the heart, muscle, and pancreas (Table 2). In the neuronal tissues, the nuclei of the motor neurons showed the most prominent diffuse nuclear staining and NIs. Glial cells also showed marked staining, but not the dorsal root ganglia. The regions with diffuse nuclear staining and NIs also showed immunoreactivity to an antibody to AR (N-20) (data not shown). Neither 1C2 nor N-20 revealed immunoreactivity in the cytoplasm. Diffuse nuclear staining and NIs were found at 4 weeks of age and became more profound with aging, although

Table 2. Distribution of Nuclear Inclusions and Diffuse Nuclear Staining with 1C2

Tissue	Male Nuclear Inclusions (NIs)/Diffuse Nuclear Staining (D)			Female Nuclear Inclusions (NIs)/Diffuse Nuclear Staining (D)		
Neuronal	Total NIs/D	Neuronal NIs/D	Glial NIs/D	Total NIs/D	Neuronal NIs/D	Glial NIs/D
Cerebral cortex	+/++	+/++	+/++	–~+/+	–~+/+	–~+/+
Olfactory bulb	+~++/++	+~++/++	+/++	–~+/+	–~+/+	–~+/+
Basal ganglia	+/++	+/++	+/++	–~+/–~+	–~+/–~+	–~+/–~+
Cerebellum	+~++/++	+/++	+~++/++	–~+/+	–~+/+	–~+/+
Pons	+/++	+/++	+/++	–~+/–~+	–~+/–~+	–~+/–~+
Ependyma	–~+/–~+			–~+/–~+		
Spinal cord	++~+++/+++	++/++~+++	++/++~+++	–~+/+	–~+/+	–~+/+
Dosal root ganglia	–~+/–~+	–~+/–~+	–/–	–~+/–~+	–~+/–~+	–/–
Non-neuronal						
Muscle	++/+			–~+/–~+		
Heart	++/+			–~+/–~+		
Pancreas	–~++/–~++			–~+/–~+		
Eye	–~+/–~+			–/–		
Lung	–~+/–~+			–/–		
Kidney	–/–			–/–		
Liver	–/–			–/–		
Stomach	–/–			–/–		
Intestine	–/–			–/–		
Spleen	–/–			–/–		
Thymus	–/–			–/–		
Skin	–/–			–/–		
Prostate	–~+					
Testis	–					
Ovary	–					

–, absent; + mild; ++, moderate; +++, abundant. In the case that the amount of NIs or D differs among three lines, we delineate its range. Three lines, #2–6, #4–6, and #7–8, were autopsied at 12, 18, 15 weeks of age, respectively.